CNES and **ILNAS**
GNSS stations relative calibration
G1/G2 #1011-2025

Michel Abgrall, Baptiste Chupin, Caroline Lim

Observatoire de Paris

`michel.abgrall@obspm.fr, baptiste.chupin@obspm.fr, caroline.lim@obspm.fr`

June 27, 2025
Issue 1.0

1 Introduction.

1.1 General informations.

This calibration report released by LNE-OP is about the G1/G2 relative calibration campaign of GNSS stations located in CNES and ILNAS. This campaign took place from 18 January 2025 (MJD 60693) to 19 March 2025 (MJD 60753).
The report is built according to the Annex 4 of the document “BIPM guidelines for GNSS calibration” [1] and contains all the required informations, data, plots and results either required by BIPM in the frame of the CCTF Working Group on GNSS, or by BIPM and EURAMET in the frame of the Group1/Group2 calibration scheme. It also contains the uncertainty budget computation according to the Guidelines, which is showing whether the calibrated links used in the frame of the TAI computation would be in line with the conventional values.
This report is consistent with the capabilities that are included in Appendix C of the CIPM MRA drawn up by the CIPM. Under the CIPM MRA, all participating institutes recognize the validity of each other’s calibration and measurement certificates for the quantities, ranges and measurement uncertainties specified in the KCDB (for details see `https://www.bipm.org/kcdb/`).
The first section of this document gives the introduction, the document structure, the list of acronyms and of the reference documents. Section 2 contains a summary of the results. Section 3 describes the equipment and operations during the calibration campaign. Section 4 provides all informations about data handling and calibration processing. Section 5 is about the calibration results between stations, and Section 6 is devoted to the uncertainty budgets computation. This document finish with an assessment of the stability of the GNSS reference station and of the traveling ones during this campaign in Section 7.
Annex A provides the required BIPM information sheets for all GNSS stations involved. Annex B shows the plots of the raw data together with the related TDEV. Annex C describes all the terms appearing in the uncertainty budgets.

1.2 Calibration report changes.

This is issue 1.0 of the calibration report

1.3 Acronym list.

ADEV:	Allan deviation, square root of AVAR
AVAR:	Allan variance or Two-sample variance
Beidou:	Chinese GNSS
BIPM:	Bureau International des Poids et Mesures
CCTF:	Consultative Committee on Time and Frequency
CGGTTS:	CCTF Global GNSS Time Transfer Standard format
CIPM:	Comité International des Poids et Mesures
CV:	Common-view
Galileo:	European Union GNSS
GFZ:	Geoforschungszentrum, Germany
GLONASS:	Russian GNSS
GNSS:	Global Navigation Satellite System
GPS:	United States of America GNSS
IGS:	International GNSS Service
LNE:	Laboratoire National de Métrologie et d'Essais, France
LNE-OP:	French designated laboratory in charge of time and frequency units
MDEV:	Modified Allan deviation, square root of MVAR
MVAR:	Modified Allan variance
NA:	Not Applicable
NMI:	National Metrology Institute
NRCan:	National Resources Canada
OP:	Observatoire de Paris, France
PPP:	Precise Point Positioning
PPS:	Pulse per second
RINEX:	Receiver international exchange format for Geodesy
LTE:	Laboratoire Temps Espace, OP laboratory where LNE-OP is located
TDEV:	Time Allan deviation, square root of TVAR
TIC:	Time Interval Counter
TVAR:	Time Allan variance

1.4 Reference documents.

[1] BIPM. *"BIPM guidelines for GNSS calibration"*. Version V4.0. 05/08/2021.

[2] G. D. Rovera, M. Abgrall, P. Uhrich, P. Defraigne, and B. Bertrand. "GNSS antenna multipath effects". In: *Proc. of the 31st European Frequency and time Forum (EFTF)*. Torino, Italy, 2018.

[3] G. D. Rovera, M. Siccardi, S. Römisch, and M. Abgrall. "Time delay measurements: estimation of the error budget". In: *Metrologia* 56.3 (2019).

[4] G. D. Rovera, M. Abgrall, P. Uhrich, and M. Siccardi. "Techniques of antenna cable delay measurement for GPS time transfer". In: *Proc. of the 5th International Colloquium on Scientific and Fundamental Aspects of the Galileo Programme*. Braunschweig, Germany, 27-29 October 2015.

[5] P. Uhrich and D. Valat. "GPS receiver relative calibration campaign preparation for Galileo In-Orbit Validation". In: *Proc. of the 24th European Frequency and time Forum (EFTF)*. Noordwijk, The Netherlands, April 2010.

[6] G. D. Rovera, J.-M. Torre, R. Sherwood, M. Abgrall, C. Courde, M. Laas-Bourez, and P. Uhrich. "Link calibration against receiver calibration: an assessment of GPS time transfer uncertainties". In: *Metrologia* 51.5 (2014), pp. 476–490.

2 Summary of the results.

This Section is a summary of the station relative calibration results. Table 1 provides the GPS P1-code and P2-code calibrated delays for CNES and ILNAS stations, from where the ionosphere-free linear combination P3 delays are computed, together with their related uncertainties according to the conventional values. Table 2 provides the corresponding results for Galileo E1-code, E5a-code calibrated and ionosphere-free combination E3. Table 3 provides the corresponding results for Beidou B1C-code, B2a-code calibrated and ionosphere-free combination B3. These results are fully valid for the period of the calibration campaign.
For CNES stations, if we compare the current results to the previous calibration performed by LNE-OP in 2021 (Cal 1012-2021), we find that the total delays are in agreement to better than 1.1 ns in P3 and to better than 1.4 ns in E3.

For ILNAS stations, if we compare the current results to the previous calibration performed by LNE-OP in 2023 (Cal 1014-2023), we find that the total delays are in agreement to better than 800 ps in P3 and to better than 400 ps in E3.

Table 1: Summary of the stations GPS delays (all values in ns)

Station	Measurement period	P1 delays	Combined uncertainty	P2 delays	Combined uncertainty	P3 delays	Combined uncertainty	Combined uncertainty [*]
CS23	60707–60711	31.294	0.6	27.858	0.6	36.605	0.9	2.5
CS24	60707–60711	34.823	0.6	31.676	0.6	39.687	0.9	2.5
LU01	60730–60737	28.170	0.6	25.062	0.6	32.974	0.9	2.5
LU02	60730–60737	30.550	0.6	27.694	0.6	34.965	0.9	2.5

Table 2: Summary of the stations Galileo delays (all values in ns)

Station	Measurement period	E1 delays	Combined uncertainty	E5a delays	Combined uncertainty	E3 delays	Combined uncertainty	Combined uncertainty [*]
CS23	60707–60711	33.340	0.6	31.713	0.6	35.391	0.8	2.5
CS24	60707–60711	36.933	0.6	38.115	0.6	35.443	0.8	2.5
LU01	60730–60737	30.636	0.6	30.974	0.6	30.210	0.8	2.5
LU02	60730–60737	32.812	0.6	31.495	0.6	34.472	0.8	2.5

Table 3: Summary of the stations Beidou delays (all values in ns)

Station	Measurement period	B1C delays	Combined uncertainty	B2a delays	Combined uncertainty	B3 delays	Combined uncertainty	Combined uncertainty [*]
CS23	60707–60711	33.036	0.6	31.140	0.6	35.426	0.8	2.5
CS24	60707–60711	36.862	0.6	37.538	0.6	36.010	0.8	2.5
LU02	60730–60737	32.440	0.6	30.972	0.6	34.291	0.8	2.5

[*] Conventional combined uncertainty value for G1/G2 calibration, including the OP reference station combined uncertainty.

3 Description of equipment.

3.1 OP GNSS equipment.

OP73 is currently made of a Septentrio multichannel multi-GNSS PolaRx5-TR, a high quality 30 m antenna cable and a SepChoke B3/E6 multi-GNSS choke-ring antenna. This station was part of the last G1 calibration campaign (# 1001-2022), its delays having been computed by BIPM with P3, E3 and B3 time transfer conventional combined uncertainties of 1.8 ns for GPS and 1.5 ns for Galileo and Beidou, respectively.
The OP GNSS traveling equipment is made of two multi-GNSS Septentrio PolaRx5-TR main units called OP72 and OP74, connected to one single 50 m long antenna cable thanks to a power splitter, and to one single multi-GNSS Veraphase 6000 antenna.
All the OP PolaRx5-TR receivers involved in this calibration are operated with the PPS-In delay compensation disabled: the PPS-Out connectors define their reference point for refdelay measurements.

3.2 UTC(k) GNSS equipment.

The UTC(k) GNSS equipment to calibrate was depending on the visited site. The receiver main units were all Septentrio PolaRx5TR, but there were different antennas. At CNES, CS23 is connected to a SEPCHOKE B3E6 antenna and CS24 to a LEICA AR20. At ILNAS both receivers are connected to two seperate SEPCHOKE B3E6 antennas. All the UTC(k) PolaRx5-TR receivers involved in this calibration are operated with the PPS-In delay compensation disabled: the PPS-Out connectors define their reference point for refdelay measurements. Annex A contains the details about the local implementations in the visited stations. These stations were calibrated as G2 GNSS stations according to the BIPM Guidelines for the delays computations including the related combined uncertainties.

3.3 Summary of the involved equipment and planning.

Table 4 summarizes the equipment involved in the GNSS relative calibration campaign with highlighted traveling station measurement periods on each site.

Table 4: Description of equipment

Institute	Status of equipement	MJD of measurement	Receiver type	BIPM code	RINEX name
OP	Traveling	NA – NA	Septentrio PolaRx5TR	OP72	OP72
OP	Traveling	NA – NA	Septentrio PolaRx5TR	OP74	OP74
OP	Groupe 1 Reference	60693 – 60698	Septentrio PolaRx5TR	OP73	OP73
OP	Groupe 1 Reference	60748 – 60753	Septentrio PolaRx5TR	OP73	OP73
CNES	Groupe 2	60707 – 60711	Septentrio PolaRx5TR	CS23	CS23
CNES	Groupe 2	60707 – 60711	Septentrio PolaRx5TR	CS24	CS24
ILNAS	Groupe 2	60730 – 60737	Septentrio PolaRx5TR	LU01	LU01
ILNAS	Groupe 2	60730 – 60737	Septentrio PolaRx5TR	LU02	LU02

4 Data and processing.

All OP collected raw Septentrio binary files (SBF) data are transformed into GNSS RINEX 3 format by using the Septentrio proprietary SBF2RIN software. Local receivers SBF and/or RINEX 3 and/or RINEX 2 data, together with CGGTTS files when they exist, are provided by the visited institution/laboratory. The calibration is consisting in building differential 30 s sampled CGGTTS data for each P1- and P2- codes for GPS, for each E1- and E5a- codes for Galileo and for each B1C- and B2a- codes for Beidou between pairs of receivers, for which we partly use the R2CGGTTS software developed by P. Defraigne (ORB). Another part of the calibration software is an original development by LNE-OP. These CGGTTS differences are corrected by the known reference delay (REFDLY) and antenna cable delay (CABDLY) when available. In this case, the calibrated delays are for the ensemble receiver main unit plus antenna.

For each location, the coordinates of the antenna phase centers are especially computed for the calibration period from RINEX 2 files by using the NRCan PPP software. Unfortunately, this computation is limited to GPS phase center for L1 and L2 carrier frequencies. Galileo E1 carrier and Beidou B1C being equal to L1, we assume the phase centers are identical. But it is not the case for Galileo E5a and Beidou B2a compared to L2, and we can only approximate the Galileo E5a and Beidou B2a phase centers by using L2 one. The geometric correction between pairs of antenna phase centers for receivers in common-clock set-up is computed by using Rapid BRDC files provided by IGS.

Reference delays are measured against either the local UTC(k) physical reference point or the local time scale reference point at the trigger level currently used in the involved laboratories. The trigger level in LNE-OP is 1.0 V. Antenna cable delay is either obtained from dedicated measurements or included in the P1 and P2 delays, in the E1 and E5a delays and in the B1C and B2a delays when no value is available for this parameter. In this latter case, the CABDLY value is set to 0 in the parameter file, and the calibrated delays are for the ensemble receiver main unit plus antenna cable plus antenna.

For validation purposes, ionosphere-free linear combinations P3, E3 and B3 CGGTTS files are computed by using the R2CGGTTS software provided by P. Defraigne (ORB), and CV are built between pairs of receivers. This is more especially the case when we are using two traveling receivers in a visited location, in order to better assess the stability of this traveling ensemble all over the calibration campaign. The conservative estimated value for the traveling equipment stability during such a campaign is typically chosen for each code as the maximum between the misclosure between the start and the end of the campaign and the average offset between both traveling receivers as measured in each location.

As conservative estimate, the noise of the P1 and P2 differences, of the E1 and E5a differences and of the B1C and B2a differences is obtained from the highest value of the one-sigma statistical uncertainty of the TDEV at 1 d, issued from a linear interpolation between consecutive TDEV points when required. In the case there is not enough data to compute a TDEV at 1 d, the upper limit of the last error bar available is considered as noise of the raw differences. The noise of P3, E3 and B3 data is issued from a similar analysis on TDEV data.

5 Results of raw data processing.

Table 5, table 6 and table 7 provide a summary of all the delays involved in the GPS codes, in the Galileo codes and in the Beidou codes, respectively. The tables provide first the calibration of the traveling stations OP72 and OP74 against the reference station OP73 at the start and the end of the campaign, from which we estimate, from an average, the internal delays to be accounted for during measurements at the remote site. Then the tables show the calibration of the visited stations against these traveling receivers. The calibration results summarized in tables 1, 2 and 3 are computed from the average delays of both traveling receivers. The misclosure was found at 130 ps or below for each GPS, Galileo and Beidou codes which demonstrates the good stability of the traveling equipment during the campaign. As typically expected, the noise estimates from the TDEVs are below 200 ps, and are hence remaining low enough in the uncertainty budgets (see Section 6). All the plots of P1, P2, E1, E5a, B1C and B2a differences are provided in Annex B, together with the related TDEV analysis. The P3, E3 and B3 computed by using the results of the calibration and the related TDEV are also made available in Annex B.

Table 5: Summary of **GPS** delays (all values in ns)

Receiver	Reference	MJD of Measurement	REFDLY	CABDLY	P1 DLY	TDEV	P2 DLY	TDEV	P3 DLY	TDEV
OP73	Ref	60693 – 60698	85.2	129.6	29.550	NA	26.020	NA	35.006	NA
OP72	OP73	60693 – 60698	93.2	0.0	224.037	0.023	221.846	0.030	227.424	0.074
OP74	OP73	60693 – 60698	111.3	0.0	224.788	0.021	222.659	0.030	228.079	0.072
OP73	Ref	60748 – 60753	85.2	129.6	29.550	NA	26.020	NA	35.006	NA
OP72	OP73	60748 – 60753	104.7	0.0	224.112	0.022	222.001	0.034	227.376	0.086
OP74	OP73	60748 – 60753	89.2	0.0	222.720	0.021	222.652	0.035	227.917	0.091
OP72	Ref	60707 – 60711	38.4	0.0	224.074	NA	221.923	NA	227.399	NA
CS23	OP72	60707 – 60711	60.0	118.3	31.272	0.034	27.840	0.040	36.577	0.080
CS24	OP72	60707 – 60711	60.1	118.5	34.801	0.053	31.657	0.017	39.661	0.120
OP74	Ref	60707 – 60711	56.2	0.0	224.754	NA	222.655	NA	227.998	NA
CS23	OP74	60707 – 60711	60.0	118.3	31.315	0.035	27.877	0.040	36.629	0.078
CS24	OP74	60707 – 60711	60.1	118.5	34.845	0.055	31.694	0.016	39.716	0.130
OP72	Ref	60730 – 60737	50.2	0.0	224.074	NA	221.923	NA	227.399	NA
LU01	OP72	60730 – 60737	36.6	117.4	28.170	0.055	25.054	0.033	32.986	0.101
LU02	OP72	60730 – 60737	38.6	160.6	30.551	0.036	27.686	0.039	34.980	0.103
OP74	Ref	60730 – 60737	68.2	0.0	224.754	NA	222.655	NA	227.998	NA
LU01	OP74	60730 – 60737	36.6	117.4	28.169	0.053	25.071	0.030	32.958	0.102
LU02	OP74	60730 – 60737	38.6	160.6	30.549	0.037	27.701	0.037	34.951	0.107

Table 6: Summary of **Galileo** delays (all values in ns)

Receiver	Reference	MJD of Measurement	REFDLY	CABDLY	E1 DLY	TDEV	E5a DLY	TDEV	E3 DLY	TDEV
OP73	Ref	60693 – 60698	85.2	129.6	31.780	NA	31.520	NA	32.108	NA
OP72	OP73	60693 – 60698	93.2	0.0	226.433	0.027	225.922	0.044	227.077	0.055
OP74	OP73	60693 – 60698	111.3	0.0	227.324	0.026	226.738	0.041	228.063	0.054
OP73	Ref	60748 – 60753	85.2	129.6	31.780	NA	31.520	NA	32.108	NA
OP72	OP73	60748 – 60753	104.7	0.0	226.407	0.035	226.039	0.040	226.871	0.077
OP74	OP73	60748 – 60753	89.2	0.0	227.157	0.037	226.702	0.041	227.731	0.079
OP72	Ref	60707 – 60711	38.4	0.0	226.420	NA	225.980	NA	226.975	NA
CS23	OP72	60707 – 60711	60.0	118.3	33.324	0.020	31.703	0.021	35.367	0.056
CS24	OP72	60707 – 60711	60.1	118.5	36.916	0.042	38.105	0.032	35.417	0.126
OP74	Ref	60707 – 60711	56.2	0.0	227.241	NA	226.720	NA	227.898	NA
CS23	OP74	60707 – 60711	60.0	118.3	33.357	0.021	31.723	0.020	35.417	0.060
CS24	OP74	60707 – 60711	60.1	118.5	36.950	0.042	38.125	0.030	35.469	0.128
OP72	Ref	60730 – 60737	50.2	0.0	226.420	NA	225.980	NA	226.975	NA
LU01	OP72	60730 – 60737	36.6	117.4	30.630	0.047	30.971	0.087	30.200	0.133
LU02	OP72	60730 – 60737	38.6	160.6	32.808	0.047	31.491	0.074	34.468	0.119
OP74	Ref	60730 – 60737	68.2	0.0	227.241	NA	226.720	NA	227.898	NA
LU01	OP74	60730 – 60737	36.6	117.4	30.643	0.045	30.978	0.088	30.221	0.130
LU02	OP74	60730 – 60737	38.6	160.6	32.817	0.048	31.499	0.072	34.478	0.119

Table 7: Summary of **Beidou** delays (all values in ns)

Receiver	Reference	MJD of Measurement	REFDLY	CABDLY	B1C DLY	TDEV	B2a DLY	TDEV	B3 DLY	TDEV
OP73	Ref	60693 – 60698	85.2	129.6	31.630	NA	30.930	NA	32.512	NA
OP72	OP73	60693 – 60698	93.2	0.0	226.230	0.036	225.348	0.029	227.342	0.089
OP74	OP73	60693 – 60698	111.3	0.0	227.213	0.034	226.164	0.028	228.535	0.085
OP73	Ref	60748 – 60753	85.2	129.6	31.630	NA	30.930	NA	32.512	NA
OP72	OP73	60748 – 60753	104.7	0.0	226.200	0.020	225.474	0.026	227.115	0.055
OP74	OP73	60748 – 60753	89.2	0.0	227.045	0.020	226.140	0.026	228.186	0.057
OP72	Ref	60707 – 60711	38.4	0.0	226.215	NA	225.411	NA	227.229	NA
CS23	OP72	60707 – 60711	60.0	118.3	33.017	0.037	31.130	0.037	35.396	0.103
CS24	OP72	60707 – 60711	60.1	118.5	36.844	0.050	37.527	0.032	35.983	0.121
OP74	Ref	60707 – 60711	56.2	0.0	227.129	NA	226.152	NA	228.361	NA
CS23	OP74	60707 – 60711	60.0	118.3	33.054	0.037	31.151	0.040	35.453	0.115
CS24	OP74	60707 – 60711	60.1	118.5	36.881	0.050	37.549	0.033	36.039	0.122
OP72	Ref	60730 – 60737	50.2	0.0	226.215	NA	225.411	NA	227.229	NA
LU02	OP72	60730 – 60737	38.6	160.6	32.430	0.044	30.968	0.068	34.273	0.073
OP74	Ref	60730 – 60737	68.2	0.0	227.129	NA	226.152	NA	228.361	NA
LU02	OP74	60730 – 60737	38.6	160.6	32.450	0.044	30.977	0.069	34.307	0.086

6 Uncertainty budgets.

Tables 8 to 18 are providing the uncertainty budget for the computed internal delays of the CNES and ILNAS stations for GPS, Galileo and Beidou, respectively. All the values are given in ns. See Annex C for detailed explanations about the different terms.
The Type A uncertainty on measured codes is estimated from the high value of the 1 sigma statistical uncertainty of the TDEV(1 d). To be conservative, we take the largest value obtained within the two traveling receivers. The Type A uncertainty of the difference between codes is the quadratic sum between both estimations. The P3, E3 and B3 Type A uncertainties are estimated from the high value of the 1 sigma statistical uncertainty of the related TDEV(1 d). All TDEV plots are in Annex B.
To estimate the misclosure, we first compute the deviation from closure between the traveling stations OP72 and OP74, and the reference station OP73 for each GNSS code. We then calculate the average of these values, taken as positive.
The GPS P3 misclosure is estimated by applying to the misclosure values computed for P1- and P2- code the ionosphere-free linear combination formula: $P3 = P1 + 1.546 \times (P1 - P2)$
The Galileo E3 misclosure is estimated by applying to the misclosure values computed for E1- and E5a- code the ionosphere-free linear combination formula:
$E3 = E1 + 1.261 \times (E1 - E5a)$
The Beidou B3 misclosure is estimated by applying to the misclosure values computed for B1C- and B2c- code the ionosphere-free linear combination formula:
$B3 = B1C + 1.261 \times (B1C - B2a)$
It was not necessary to measure separately the antenna cable delays (CABDLY) of the traveling equipment which remained in the same configuration at OP and at the visited site. Therefore the corresponding uncertainties are expected to be negligible.
The delay of the antenna cables of the CNES and ILNAS stations has not been measured. Calibration was done using prior antenna cable delay measurement values, provided by the visited laboratories. There is therefore no uncertainty associated with the antenna cable. The uncertainty of the calibrations correspond to that of the overall calibrations (internal delay + antenna + antenna cable).

Table 8: **CS23** uncertainty budget for **GPS** calibrated delays (all values in ns)

Uncertainty type	P1	P2	P1-P2	P3	Description
u_a(Reference)	0.023	0.035	0.042	0.091	Largest TDEV(1 d) sigma between the start and the end of OP72 or OP74 against OP73
u_a(CS23)	0.035	0.040	0.054	0.080	Largest TDEV(1 d) sigma of offset between visited station and OP72 or OP74
Type A uncertainties					
u_a	0.042	0.054	0.069	0.122	Visited against reference
Misclosure					
$u_{b,1}$	0.072	0.082	0.011	0.056	Actual misclosure offset
Systematic components related to RAWDIF					
$u_{b,11}$	0.070	0.070	0.099	0.168	Position error at OP
$u_{b,12}$	0.070	0.070	0.099	0.168	Position error at visited site
$u_{b,13}$	0.200	0.200	0.283	0.481	Multipaths at OP
$u_{b,14}$	0.200	0.200	0.283	0.481	Multipaths at visited site
Link of the traveling system to local time scale					
$u_{b,21}$	0.220	0.220		0.220	REFDLY at OP
$u_{b,22}$	0.220	0.220		0.220	REFDLY at visited site
Link of the reference system to UTC(OP)					
$u_{b,31}$	0.220	0.220		0.220	REFDLY at OP
Link of the visited system to its local time scale					
$u_{b,32}$	0.220	0.220		0.220	REFDLY at visited site
Antenna cable delays of the traveling system					
$u_{b,41}$	0.000	0.000		0.000	CABDLY at OP
$u_{b,42}$	0.000	0.000		0.000	CABDLY at visited site
Antenna cable delays of the visited system					
$u_{b,43}$	0.000	0.000		0.000	CABDLY at visited site
Type B uncertainties					
$u_{b,SYS}$	0.538	0.539		0.846	Quadratic sum of u_b
Combined uncertainties					
u_{CAL0}	0.540	0.542		0.855	Composed of u_a and $u_{b,SYS}$

Table 9: **CS24** uncertainty budget for **GPS** calibrated delays (all values in ns)

Uncertainty type	P1	P2	P1-P2	P3	Description
u_a(Reference)	0.023	0.035	0.042	0.091	Largest TDEV(1 d) sigma between the start and the end of OP72 or OP74 against OP73
u_a(CS24)	0.055	0.017	0.058	0.130	Largest TDEV(1 d) sigma of offset between visited station and OP72 or OP74
Type A uncertainties					
u_a	0.060	0.039	0.072	0.159	Visited against reference
Misclosure					
$u_{b,1}$	0.072	0.082	0.011	0.056	Actual misclosure offset
Systematic components related to RAWDIF					
$u_{b,11}$	0.070	0.070	0.099	0.168	Position error at OP
$u_{b,12}$	0.070	0.070	0.099	0.168	Position error at visited site
$u_{b,13}$	0.200	0.200	0.283	0.481	Multipaths at OP
$u_{b,14}$	0.200	0.200	0.283	0.481	Multipaths at visited site
Link of the traveling system to local time scale					
$u_{b,21}$	0.220	0.220		0.220	REFDLY at OP
$u_{b,22}$	0.220	0.220		0.220	REFDLY at visited site
Link of the reference system to UTC(OP)					
$u_{b,31}$	0.220	0.220		0.220	REFDLY at OP
Link of the visited system to its local time scale					
$u_{b,32}$	0.220	0.220		0.220	REFDLY at visited site
Antenna cable delays of the traveling system					
$u_{b,41}$	0.000	0.000		0.000	CABDLY at OP
$u_{b,42}$	0.000	0.000		0.000	CABDLY at visited site
Antenna cable delays of the visited system					
$u_{b,43}$	0.000	0.000		0.000	CABDLY at visited site
Type B uncertainties					
$u_{b,SYS}$	0.538	0.539		0.846	Quadratic sum of u_b
Combined uncertainties					
u_{CAL0}	0.542	0.541		0.861	Composed of u_a and $u_{b,SYS}$

Table 10: **LU01** uncertainty budget for **GPS** calibrated delays (all values in ns)

Uncertainty type	P1	P2	P1-P2	P3	Description
u_a(Reference)	0.023	0.035	0.042	0.091	Largest TDEV(1 d) sigma between the start and the end of OP72 or OP74 against OP73
u_a(LU01)	0.055	0.033	0.065	0.102	Largest TDEV(1 d) sigma of offset between visited station and OP72 or OP74
Type A uncertainties					
u_a	0.060	0.049	0.078	0.137	Visited against reference
Misclosure					
$u_{b,1}$	0.072	0.082	0.011	0.056	Actual misclosure offset
Systematic components related to RAWDIF					
$u_{b,11}$	0.070	0.070	0.099	0.168	Position error at OP
$u_{b,12}$	0.070	0.070	0.099	0.168	Position error at visited site
$u_{b,13}$	0.200	0.200	0.283	0.481	Multipaths at OP
$u_{b,14}$	0.200	0.200	0.283	0.481	Multipaths at visited site
Link of the traveling system to local time scale					
$u_{b,21}$	0.220	0.220		0.220	REFDLY at OP
$u_{b,22}$	0.220	0.220		0.220	REFDLY at visited site
Link of the reference system to UTC(OP)					
$u_{b,31}$	0.220	0.220		0.220	REFDLY at OP
Link of the visited system to its local time scale					
$u_{b,32}$	0.220	0.220		0.220	REFDLY at visited site
Antenna cable delays of the traveling system					
$u_{b,41}$	0.000	0.000		0.000	CABDLY at OP
$u_{b,42}$	0.000	0.000		0.000	CABDLY at visited site
Antenna cable delays of the visited system					
$u_{b,43}$	0.000	0.000		0.000	CABDLY at visited site
Type B uncertainties					
$u_{b,SYS}$	0.538	0.539		0.846	Quadratic sum of u_b
Combined uncertainties					
u_{CAL0}	0.542	0.542		0.858	Composed of u_a and $u_{b,SYS}$

Table 11: **LU02** uncertainty budget for **GPS** calibrated delays (all values in ns)

Uncertainty type	P1	P2	P1-P2	P3	Description
u_a(Reference)	0.023	0.035	0.042	0.091	Largest TDEV(1 d) sigma between the start and the end of OP72 or OP74 against OP73
u_a(LU02)	0.037	0.039	0.054	0.107	Largest TDEV(1 d) sigma of offset between visited station and OP72 or OP74
Type A uncertainties					
u_a	0.044	0.053	0.069	0.141	Visited against reference
Misclosure					
$u_{b,1}$	0.072	0.082	0.011	0.056	Actual misclosure offset
Systematic components related to RAWDIF					
$u_{b,11}$	0.070	0.070	0.099	0.168	Position error at OP
$u_{b,12}$	0.070	0.070	0.099	0.168	Position error at visited site
$u_{b,13}$	0.200	0.200	0.283	0.481	Multipaths at OP
$u_{b,14}$	0.200	0.200	0.283	0.481	Multipaths at visited site
Link of the traveling system to local time scale					
$u_{b,21}$	0.220	0.220		0.220	REFDLY at OP
$u_{b,22}$	0.220	0.220		0.220	REFDLY at visited site
Link of the reference system to UTC(OP)					
$u_{b,31}$	0.220	0.220		0.220	REFDLY at OP
Link of the visited system to its local time scale					
$u_{b,32}$	0.220	0.220		0.220	REFDLY at visited site
Antenna cable delays of the traveling system					
$u_{b,41}$	0.000	0.000		0.000	CABDLY at OP
$u_{b,42}$	0.000	0.000		0.000	CABDLY at visited site
Antenna cable delays of the visited system					
$u_{b,43}$	0.000	0.000		0.000	CABDLY at visited site
Type B uncertainties					
$u_{b,SYS}$	0.538	0.539		0.846	Quadratic sum of u_b
Combined uncertainties					
u_{CAL0}	0.540	0.542		0.858	Composed of u_a and $u_{b,SYS}$

Table 12: **CS23** uncertainty budget for **Galileo** calibrated delays (all values in ns)

Uncertainty type	E1	E5a	E1-E5a	E3	Description
u_a(Reference)	0.037	0.044	0.057	0.079	Largest TDEV(1 d) sigma between the start and the end of OP72 or OP74 against OP73
u_a(CS23)	0.021	0.021	0.030	0.060	Largest TDEV(1 d) sigma of offset between visited station and OP72 or OP74
Type A uncertainties					
u_a	0.043	0.049	0.065	0.100	Visited against reference
Misclosure					
$u_{b,1}$	0.097	0.076	0.021	0.122	Actual misclosure offset
Systematic components related to RAWDIF					
$u_{b,11}$	0.070	0.070	0.099	0.143	Position error at OP
$u_{b,12}$	0.070	0.070	0.099	0.143	Position error at visited site
$u_{b,13}$	0.200	0.200	0.283	0.409	Multipaths at OP
$u_{b,14}$	0.200	0.200	0.283	0.409	Multipaths at visited site
Link of the traveling system to local time scale					
$u_{b,21}$	0.220	0.220		0.220	REFDLY at OP
$u_{b,22}$	0.220	0.220		0.220	REFDLY at visited site
Link of the reference system to UTC(OP)					
$u_{b,31}$	0.220	0.220		0.220	REFDLY at OP
Link of the visited system to its local time scale					
$u_{b,32}$	0.220	0.220		0.220	REFDLY at visited site
Antenna cable delays of the traveling system					
$u_{b,41}$	0.000	0.000		0.000	CABDLY at OP
$u_{b,42}$	0.000	0.000		0.000	CABDLY at visited site
Antenna cable delays of the visited system					
$u_{b,43}$	0.000	0.000		0.000	CABDLY at visited site
Type B uncertainties					
$u_{b,SYS}$	0.542	0.538		0.764	Quadratic sum of u_b
Combined uncertainties					
u_{CAL0}	0.544	0.541		0.771	Composed of u_a and $u_{b,SYS}$

Table 13: **CS24** uncertainty budget for **Galileo** calibrated delays (all values in ns)

Uncertainty type	E1	E5a	E1-E5a	E3	Description
u_a(Reference)	0.037	0.044	0.057	0.079	Largest TDEV(1 d) sigma between the start and the end of OP72 or OP74 against OP73
u_a(CS24)	0.042	0.032	0.053	0.128	Largest TDEV(1 d) sigma of offset between visited station and OP72 or OP74
Type A uncertainties					
u_a	0.056	0.055	0.078	0.151	Visited against reference
Misclosure					
$u_{b,1}$	0.097	0.076	0.021	0.122	Actual misclosure offset
Systematic components related to RAWDIF					
$u_{b,11}$	0.070	0.070	0.099	0.143	Position error at OP
$u_{b,12}$	0.070	0.070	0.099	0.143	Position error at visited site
$u_{b,13}$	0.200	0.200	0.283	0.409	Multipaths at OP
$u_{b,14}$	0.200	0.200	0.283	0.409	Multipaths at visited site
Link of the traveling system to local time scale					
$u_{b,21}$	0.220	0.220		0.220	REFDLY at OP
$u_{b,22}$	0.220	0.220		0.220	REFDLY at visited site
Link of the reference system to UTC(OP)					
$u_{b,31}$	0.220	0.220		0.220	REFDLY at OP
Link of the visited system to its local time scale					
$u_{b,32}$	0.220	0.220		0.220	REFDLY at visited site
Antenna cable delays of the traveling system					
$u_{b,41}$	0.000	0.000		0.000	CABDLY at OP
$u_{b,42}$	0.000	0.000		0.000	CABDLY at visited site
Antenna cable delays of the visited system					
$u_{b,43}$	0.000	0.000		0.000	CABDLY at visited site
Type B uncertainties					
$u_{b,SYS}$	0.542	0.538		0.764	Quadratic sum of u_b
Combined uncertainties					
u_{CAL0}	0.545	0.541		0.779	Composed of u_a and $u_{b,SYS}$

Table 14: **LU01** uncertainty budget for **Galileo** calibrated delays (all values in ns)

Uncertainty type	E1	E5a	E1-E5a	E3	Description
u_a(Reference)	0.037	0.044	0.057	0.079	Largest TDEV(1 d) sigma between the start and the end of OP72 or OP74 against OP73
u_a(LU01)	0.047	0.088	0.100	0.133	Largest TDEV(1 d) sigma of offset between visited station and OP72 or OP74
Type A uncertainties					
u_a	0.060	0.099	0.116	0.155	Visited against reference
Misclosure					
$u_{b,1}$	0.097	0.076	0.021	0.122	Actual misclosure offset
Systematic components related to RAWDIF					
$u_{b,11}$	0.070	0.070	0.099	0.143	Position error at OP
$u_{b,12}$	0.070	0.070	0.099	0.143	Position error at visited site
$u_{b,13}$	0.200	0.200	0.283	0.409	Multipaths at OP
$u_{b,14}$	0.200	0.200	0.283	0.409	Multipaths at visited site
Link of the traveling system to local time scale					
$u_{b,21}$	0.220	0.220		0.220	REFDLY at OP
$u_{b,22}$	0.220	0.220		0.220	REFDLY at visited site
Link of the reference system to UTC(OP)					
$u_{b,31}$	0.220	0.220		0.220	REFDLY at OP
Link of the visited system to its local time scale					
$u_{b,32}$	0.220	0.220		0.220	REFDLY at visited site
Antenna cable delays of the traveling system					
$u_{b,41}$	0.000	0.000		0.000	CABDLY at OP
$u_{b,42}$	0.000	0.000		0.000	CABDLY at visited site
Antenna cable delays of the visited system					
$u_{b,43}$	0.000	0.000		0.000	CABDLY at visited site
Type B uncertainties					
$u_{b,SYS}$	0.542	0.538		0.764	Quadratic sum of u_b
Combined uncertainties					
u_{CAL0}	0.546	0.548		0.780	Composed of u_a and $u_{b,SYS}$

Table 15: **LU02** uncertainty budget for **Galileo** calibrated delays (all values in ns)

Uncertainty type	E1	E5a	E1-E5a	E3	Description
u_a(Reference)	0.037	0.044	0.057	0.079	Largest TDEV(1 d) sigma between the start and the end of OP72 or OP74 against OP73
u_a(LU02)	0.048	0.074	0.089	0.119	Largest TDEV(1 d) sigma of offset between visited station and OP72 or OP74
Type A uncertainties					
u_a	0.061	0.087	0.106	0.143	Visited against reference
Misclosure					
$u_{b,1}$	0.097	0.076	0.021	0.122	Actual misclosure offset
Systematic components related to RAWDIF					
$u_{b,11}$	0.070	0.070	0.099	0.143	Position error at OP
$u_{b,12}$	0.070	0.070	0.099	0.143	Position error at visited site
$u_{b,13}$	0.200	0.200	0.283	0.409	Multipaths at OP
$u_{b,14}$	0.200	0.200	0.283	0.409	Multipaths at visited site
Link of the traveling system to local time scale					
$u_{b,21}$	0.220	0.220		0.220	REFDLY at OP
$u_{b,22}$	0.220	0.220		0.220	REFDLY at visited site
Link of the reference system to UTC(OP)					
$u_{b,31}$	0.220	0.220		0.220	REFDLY at OP
Link of the visited system to its local time scale					
$u_{b,32}$	0.220	0.220		0.220	REFDLY at visited site
Antenna cable delays of the traveling system					
$u_{b,41}$	0.000	0.000		0.000	CABDLY at OP
$u_{b,42}$	0.000	0.000		0.000	CABDLY at visited site
Antenna cable delays of the visited system					
$u_{b,43}$	0.000	0.000		0.000	CABDLY at visited site
Type B uncertainties					
$u_{b,SYS}$	0.542	0.538		0.764	Quadratic sum of u_b
Combined uncertainties					
u_{CAL0}	0.546	0.545		0.778	Composed of u_a and $u_{b,SYS}$

Table 16: **CS23** uncertainty budget for **Beidou** calibrated delays (all values in ns)

Uncertainty type	B1C	B2a	B1C-B2a	B3	Description
u_a(Reference)	0.036	0.029	0.046	0.089	Largest TDEV(1 d) sigma between the start and the end of OP72 or OP74 against OP73
u_a(CS23)	0.037	0.040	0.055	0.115	Largest TDEV(1 d) sigma of offset between visited station and OP72 or OP74
Type A uncertainties					
u_a	0.052	0.050	0.072	0.146	Visited against reference
Misclosure					
$u_{b,1}$	0.099	0.076	0.024	0.129	Actual misclosure offset
Systematic components related to RAWDIF					
$u_{b,11}$	0.070	0.070	0.099	0.143	Position error at OP
$u_{b,12}$	0.070	0.070	0.099	0.143	Position error at visited site
$u_{b,13}$	0.200	0.200	0.283	0.409	Multipaths at OP
$u_{b,14}$	0.200	0.200	0.283	0.409	Multipaths at visited site
Link of the traveling system to local time scale					
$u_{b,21}$	0.220	0.220		0.220	REFDLY at OP
$u_{b,22}$	0.220	0.220		0.220	REFDLY at visited site
Link of the reference system to UTC(OP)					
$u_{b,31}$	0.220	0.220		0.220	REFDLY at OP
Link of the visited system to its local time scale					
$u_{b,32}$	0.220	0.220		0.220	REFDLY at visited site
Antenna cable delays of the traveling system					
$u_{b,41}$	0.000	0.000		0.000	CABDLY at OP
$u_{b,42}$	0.000	0.000		0.000	CABDLY at visited site
Antenna cable delays of the visited system					
$u_{b,43}$	0.000	0.000		0.000	CABDLY at visited site
Type B uncertainties					
$u_{b,SYS}$	0.542	0.538		0.766	Quadratic sum of u_b
Combined uncertainties					
u_{CAL0}	0.545	0.541		0.780	Composed of u_a and $u_{b,SYS}$

Table 17: **CS24** uncertainty budget for **Beidou** calibrated delays (all values in ns)

Uncertainty type	B1C	B2a	B1C-B2a	B3	Description
u_a(Reference)	0.036	0.029	0.046	0.089	Largest TDEV(1 d) sigma between the start and the end of OP72 or OP74 against OP73
u_a(CS24)	0.050	0.033	0.060	0.122	Largest TDEV(1 d) sigma of offset between visited station and OP72 or OP74
Type A uncertainties					
u_a	0.062	0.044	0.076	0.152	Visited against reference
Misclosure					
$u_{b,1}$	0.099	0.076	0.024	0.129	Actual misclosure offset
Systematic components related to RAWDIF					
$u_{b,11}$	0.070	0.070	0.099	0.143	Position error at OP
$u_{b,12}$	0.070	0.070	0.099	0.143	Position error at visited site
$u_{b,13}$	0.200	0.200	0.283	0.409	Multipaths at OP
$u_{b,14}$	0.200	0.200	0.283	0.409	Multipaths at visited site
Link of the traveling system to local time scale					
$u_{b,21}$	0.220	0.220		0.220	REFDLY at OP
$u_{b,22}$	0.220	0.220		0.220	REFDLY at visited site
Link of the reference system to UTC(OP)					
$u_{b,31}$	0.220	0.220		0.220	REFDLY at OP
Link of the visited system to its local time scale					
$u_{b,32}$	0.220	0.220		0.220	REFDLY at visited site
Antenna cable delays of the traveling system					
$u_{b,41}$	0.000	0.000		0.000	CABDLY at OP
$u_{b,42}$	0.000	0.000		0.000	CABDLY at visited site
Antenna cable delays of the visited system					
$u_{b,43}$	0.000	0.000		0.000	CABDLY at visited site
Type B uncertainties					
$u_{b,SYS}$	0.542	0.538		0.766	Quadratic sum of u_b
Combined uncertainties					
u_{CAL0}	0.546	0.540		0.781	Composed of u_a and $u_{b,SYS}$

Table 18: **LU02** uncertainty budget for **Beidou** calibrated delays (all values in ns)

Uncertainty type	B1C	B2a	B1C-B2a	B3	Description
u_a(Reference)	0.036	0.029	0.046	0.089	Largest TDEV(1 d) sigma between the start and the end of OP72 or OP74 against OP73
u_a(LU02)	0.044	0.069	0.082	0.086	Largest TDEV(1 d) sigma of offset between visited station and OP72 or OP74
Type A uncertainties					
u_a	0.057	0.075	0.095	0.124	Visited against reference
Misclosure					
$u_{b,1}$	0.099	0.076	0.024	0.129	Actual misclosure offset
Systematic components related to RAWDIF					
$u_{b,11}$	0.070	0.070	0.099	0.143	Position error at OP
$u_{b,12}$	0.070	0.070	0.099	0.143	Position error at visited site
$u_{b,13}$	0.200	0.200	0.283	0.409	Multipaths at OP
$u_{b,14}$	0.200	0.200	0.283	0.409	Multipaths at visited site
Link of the traveling system to local time scale					
$u_{b,21}$	0.220	0.220		0.220	REFDLY at OP
$u_{b,22}$	0.220	0.220		0.220	REFDLY at visited site
Link of the reference system to UTC(OP)					
$u_{b,31}$	0.220	0.220		0.220	REFDLY at OP
Link of the visited system to its local time scale					
$u_{b,32}$	0.220	0.220		0.220	REFDLY at visited site
Antenna cable delays of the traveling system					
$u_{b,41}$	0.000	0.000		0.000	CABDLY at OP
$u_{b,42}$	0.000	0.000		0.000	CABDLY at visited site
Antenna cable delays of the visited system					
$u_{b,43}$	0.000	0.000		0.000	CABDLY at visited site
Type B uncertainties					
$u_{b,SYS}$	0.542	0.538		0.766	Quadratic sum of u_b
Combined uncertainties					
u_{CAL0}	0.545	0.544		0.776	Composed of u_a and $u_{b,SYS}$

7 Validation of the result.

7.1 Stability of the reference station.

The reference station in OP was based on a Septentrio PolaRx5TR receiver called OP73. Figure 1 is showing a plot which demonstrate the stability of this GNSS station during the calibration campaign. The plot is the daily averaged offset between the TWSDRR technique (Two-Way Satellite Time and Frequency Transfer, with Satre modem emision and Software Defined Radio reception) between OP and PTB, and the GNSS Common View (CV) time transfer using P3 GPS or E3 Galileo data between OP and PTB, based on OP73 in OP side and on PTBB in PTB side. In both laboratories, the signal source is a UTC(k) time scale: UTC(OP) and UTC(PTB). In this computation, the time scales being cancelled, what remains is only the offset between the two time transfer techniques.

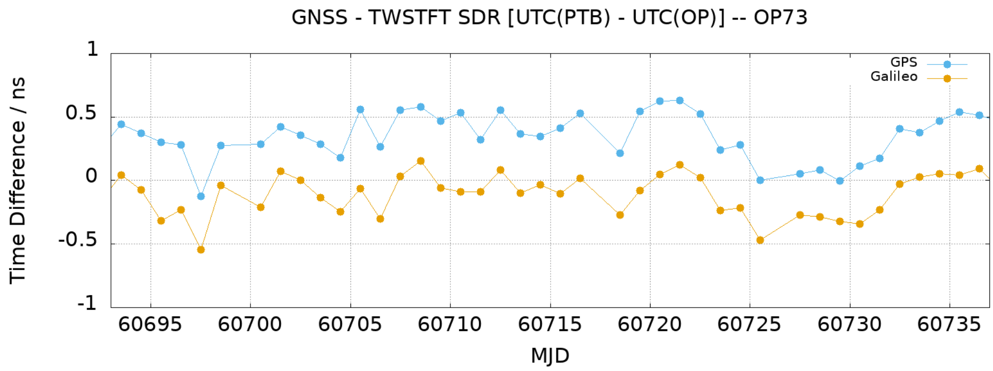

Figure 1: Daily averaged offset between TWSDRR and GPS P3 or Galileo E3 CV on the link OP-PTB during the calibration campaign.

This access the excellent stability of OP73 reference station and the consistency of the TAI network. We estimate that any potential effect of OP73 on this calibration campaign can be disregarded with respect to the final uncertainty of the calibration.

7.2 Offset between the two traveling receivers.

Figure 2, Figure 3 and Figure 4 are showing the offset between the two traveling receivers during the whole calibration campaign, based on CV between CGGTTS P3 (GPS), E3 (Galileo) and B3 (Beidou) data, by using for OP72 and OP74 the average delays computed against OP73 between the start and the closure of the campaign. The average offsets between the receivers before, during and after the trip, are lower than 60 ps, with a standard deviation below 120 ps. The traveling equipment remained very stable during the calibration campaign. We can consider that the effect of these offsets on the calibration results have a limitted impact.

Table 19: Average P3 offsets between OP72 and OP74 during the calibration (all values in ns)

Institute	ΔP3	Uncertainty
OP	−0.003	0.090
OP	0.002	0.087
CNES	−0.054	0.087
ILNAS	0.018	0.115

Table 20: Average E3 offsets between OP72 and OP74 during the calibration (all values in ns)

Institute	ΔE3	Uncertainty
OP	0.003	0.046
OP	−0.001	0.045
CNES	−0.051	0.048
ILNAS	−0.012	0.063

Figure 2: Offset between OP72 and OP74 during the calibration, based on CGGTTS P3 CV data

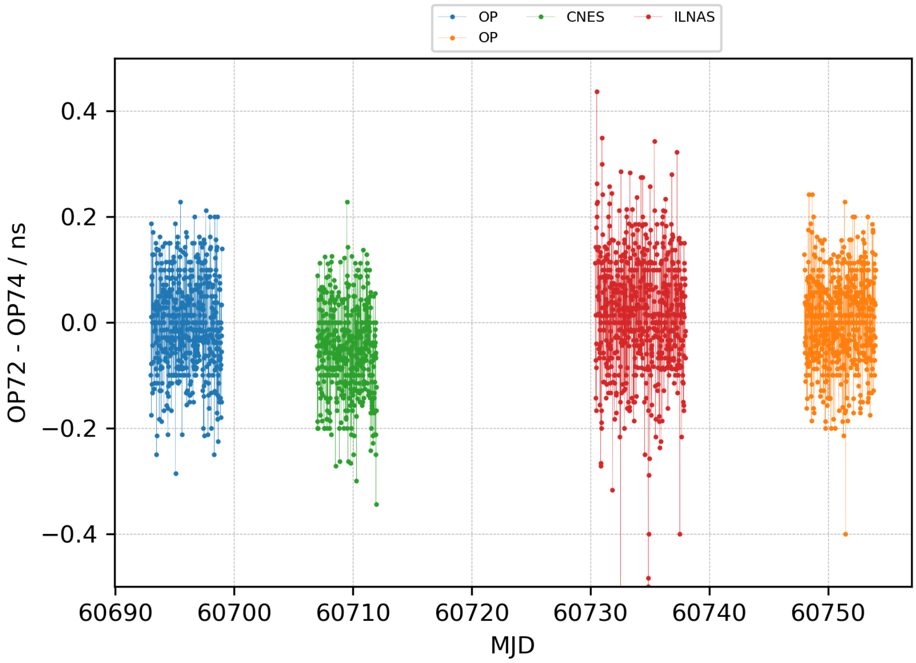

Table 21: Average B3 offsets between OP72 and OP74 during the calibration (all values in ns)

Institute	ΔB3	Uncertainty
OP	0.003	0.048
OP	0.001	0.051
CNES	−0.056	0.050
ILNAS	−0.024	0.078

Figure 3: Offset between OP72 and OP74 during the calibration, based on CGGTTS E3 CV data

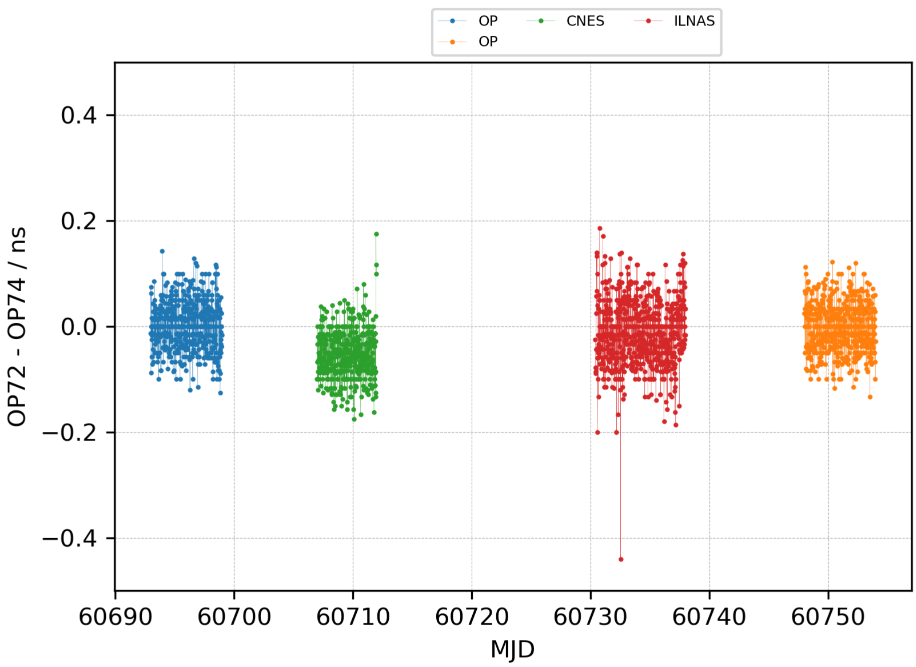

Figure 4: Offset between OP72 and OP74 during the calibration, based on CGGTTS B3 CV data

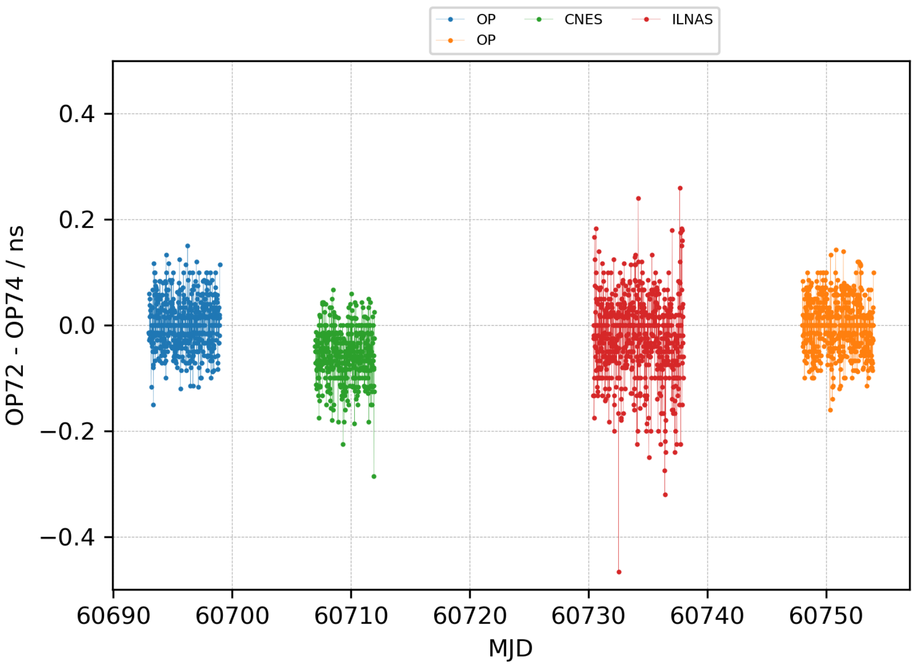

A Annex A: BIPM information sheet.

A.1 Implementation in OP.

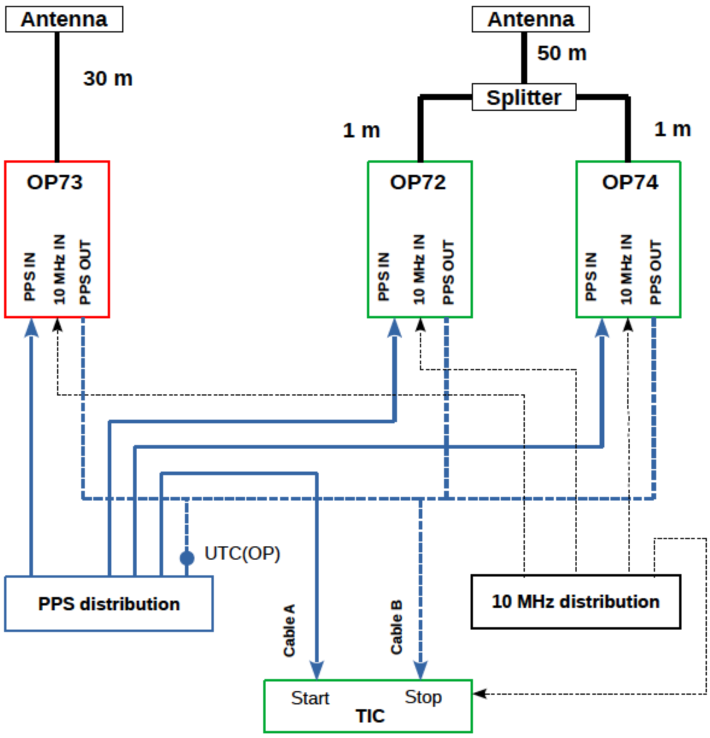

Figure 5: Implementation of OP traveling equipment in OP

A.2 Implementation in CNES.

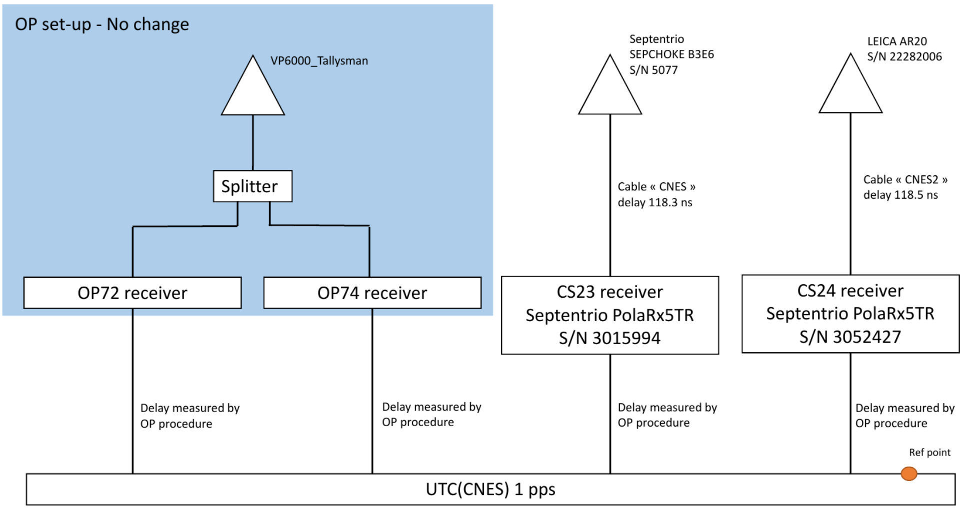

Figure 6: Implementation of CNES equipment

A.3 Implementation in ILNAS.

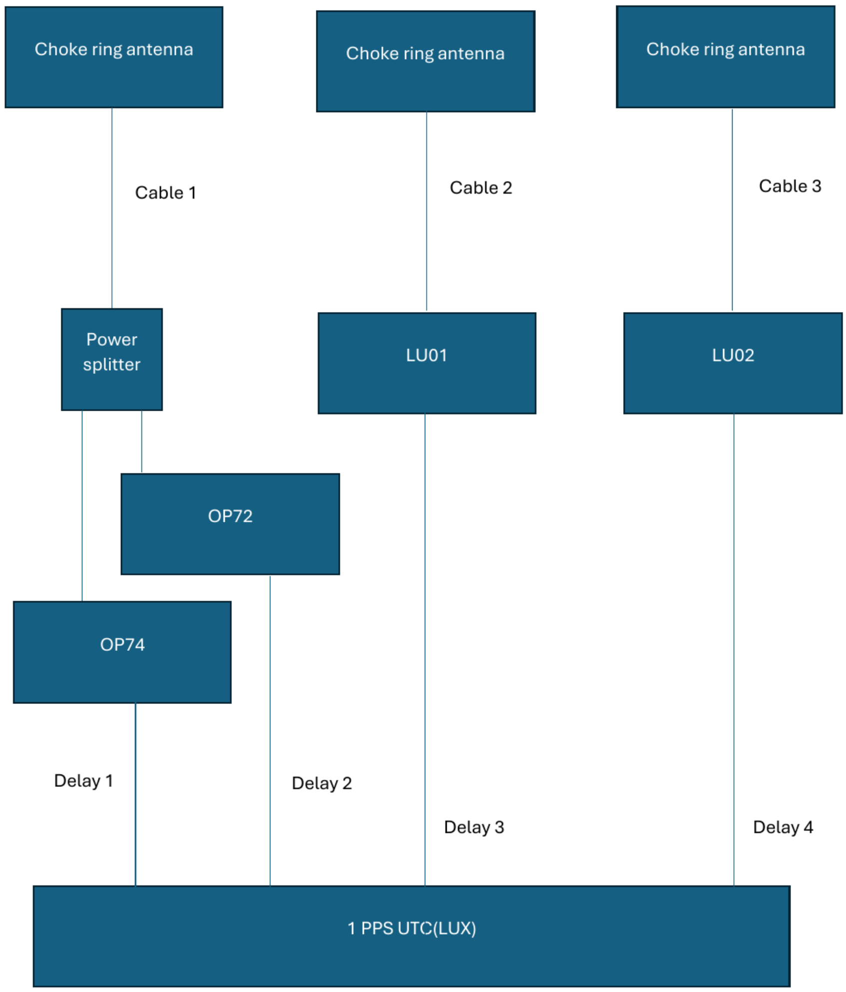

Cable 1 = ... ns (in the case it would not be the one provided in the traveling box)
Delay 1 [OP74] = 12.118 ns, Delay 2 [OP72] = 12.128 ns
Cable 2 [LU01] = 117.4 ns, Cable 3 [LU02] = 160.63 ns
Delay 3 [LU01] = 2.03 ns, Delay 4 [LU02] = 1.53 ns

Figure 7: Implementation of ILNAS equipment

Cal Id: 1011-2025 Version / Date: 10/04/2025

BIPM Information sheet

Laboratory	OP (Open)		
Date and hour beginning of measurements	18/01/2025 00:00:00		
Date and hour end measurements	23/01/2025 23:30:00		
Information on the system			
	Local	**Traveling**	
4-Character BIPM code	OP73	OP72	OP74
Receiver maker and type	PolaRx5TR	PolaRx5TR	PolaRx5TR
Receiver serial number	3069470	3069829	3069591
1 PPS triger level / V	1	1	1
Antenna cable marker and type		HY 400 UF	HY 400 UF
Phase stabilized cable (Y/N)	N	N	N
Cable length outside building / m	20	20	20
Antenna maker and type	SEPCHOKE_B3E6	TWIVP6000	TWIVP6000
Antenna serial number	5769	33-685000-01-01	33-685000-01-01
Temperature if stabilized / °C			
Mesured delays / ns			
	Local	**Traveling**	
Delay from local UTC(k) to receiver 1 PPS_IN			
Delay from 1 PPS_IN to internal reference (see Annex 1)	Compensation disabled	Compensation disabled	Compensation disabled
Antenna cable delay			
Splitter delay			
Additional cable delay			
Data used for the generation of CGGTTS files			
	Local	**Traveling**	
INT DLY (GPS) / ns	P1: 29.55 P2: 26.02	P1: 224.037 P2: 221.846	P1: 224.788 P2: 22.659
INT DLY (Galileo) / ns	E1: 31.78 E5a: 31.52	E1: 226.433 E5a: 225.922	E1: 227.324 E5a: 226.738
INT DLY (Beidou) / ns	B1c: 31.63 B2a: 30.93	B1c: 226.230 B2a: 225.348	B1c: 227.213 B2a: 226.164
CAB DLY / ns	129.6	0.0	0.0
REF DLY / ns	85.2	93.2	111.3
Coordinate reference frame	ITRF	ITRF	ITRF
Latitude or X / m	4202777.071	4202781.399	4202781.399
Longitude or Y / m	171367.028	171369.396	171369.396
Height or Z / m	4778661.392	4778659.072	4778659.072
General Information			
Rise time of local UTC pulse	500 ps		
Air conditioning (Y/N)	Y		
Set temperature value and uncertainty	22+/-1°C		
Set humidity value and uncertainty	NA		

Cal Id: 1011-2025 Version / Date: 10/04/2025

BIPM Information sheet

Laboratory	OP (Close)		
Date and hour beginning of measurements	14/03/2025 00:00:00		
Date and hour end measurements	19/03/2025 23:30:00		
Information on the system			
	Local	**Traveling**	
4-Character BIPM code	OP73	OP72	OP74
Receiver maker and type	PolaRx5TR	PolaRx5TR	PolaRx5TR
Receiver serial number	3069470	3069829	3069591
1 PPS triger level / V	1	1	1
Antenna cable marker and type		HY 400 UF	HY 400 UF
Phase stabilized cable (Y/N)	N	N	N
Cable length outside building / m	20	20	20
Antenna maker and type	SEPCHOKE_B3E6	TWIVP6000	TWIVP6000
Antenna serial number	5769	33-685000-01-01	33-685000-01-01
Temperature if stabilized / °C			
Mesured delays / ns			
	Local	**Traveling**	
Delay from local UTC(k) to receiver 1 PPS_IN			
Delay from 1 PPS_IN to internal reference (see Annex 1)	Compensation disabled	Compensation disabled	Compensation disabled
Antenna cable delay			
Splitter delay			
Additional cable delay			
Data used for the generation of CGGTTS files			
	Local	**Traveling**	
INT DLY (GPS) / ns	P1: 29.55 P2: 26.02	P1: 224.112 P2: 222.001	P1: 224.720 P2: 222.652
INT DLY (Galileo) / ns	E1: 31.78 E5a: 31.52	E1: 226.407 E5a: 226.039	E1: 227.157 E5a: 226.702
INT DLY (Beidou) / ns	B1c: 31.63 B2a: 30.93	B1c: 226.200 B2a: 225.474	B1c: 227.045 B2a: 226.140
CAB DLY / ns	129.6	0.0	0.0
REF DLY / ns	85.2	104.7	89.2
Coordinate reference frame	ITRF	ITRF	ITRF
Latitude or X / m	4202777.071	4202781.368	4202781.368
Longitude or Y / m	171367.028	171369.375	171369.375
Height or Z / m	4778661.392	4778659.048	4778659.048
General Information			
Rise time of local UTC pulse	500 ps		
Air conditioning (Y/N)	Y		
Set temperature value and uncertainty	22+/-1°C		
Set humidity value and uncertainty	NA		

Cal Id: 1011-2025 Version / Date: 24/06/2025

BIPM Information sheet

Laboratory	CNES		
Date and hour beginning of measurements	60706		
Date and hour end measurements	60712		
Information on the system			
	Local	**Traveling**	
4-Character BIPM code	CS23	OP72	OP74
Receiver maker and type	PolaRx5TR	PolaRx5TR	PolaRx5TR
Receiver serial number	3015994	3069829	3069591
1 PPS triger level / V	1	1	1
Antenna cable marker and type	LMR-400 type	HY 400 UF	HY 400 UF
Phase stabilized cable (Y/N)	Y	N	N
Cable length outside building / m	10	20	20
Antenna maker and type	SEPCHOKE_B3E6	TWIVP6000	TWIVP6000
Antenna serial number	5077	33-685000-01-01	33-685000-01-01
Temperature if stabilized / °C	no		
Mesured delays / ns			
	Local	**Traveling**	
Delay from local UTC(k) to receiver 1 PPS_IN			
Delay from 1 PPS_IN to internal reference (see Annex 1)	Compensation disabled	Compensation disabled	Compensation disabled
Antenna cable delay	118.3 ns		
Splitter delay	na		
Additional cable delay	na		
Data used for the generation of CGGTTS files			
	Local	**Traveling**	
INT DLY (GPS) / ns	P1: 31.294 P2: 27.858	P1: 224.074 P2: 221.923	P1: 224.754 P2: 222.655
INT DLY (Galileo) / ns	E1: 33.340 E5a: 31.713	E1: 226.420 E5a: 225.980	E1: 227.241 E5a: 226.720
INT DLY (Beidou) / ns	B1c: 33.036 B2a: 31.140	B1c: 226.215 B2a: 225.411	B1c: 227.129 B2a: 226.152
CAB DLY / ns	118.3	0.0	0.0
REF DLY / ns	60.0	38.4	56.2
Coordinate reference frame	ITRF	ITRF	ITRF
Latitude or X / m	4627898.510	4627901.922	4627901.922
Longitude or Y / m	119892.856	119896.445	119896.445
Height or Z / m	4372943.213	4372939.828	4372939.828
General Information			
Rise time of local UTC pulse	0.5 ns		
Air conditioning (Y/N)	Y		
Set temperature value and uncertainty	22+/-1°C		
Set humidity value and uncertainty			

Cal Id: 1011-2025 Version / Date: 24/06/2025

BIPM Information sheet

Laboratory	CNES		
Date and hour beginning of measurements	60706		
Date and hour end measurements	60712		
Information on the system			
	Local	**Traveling**	
4-Character BIPM code	CS24	OP72	OP74
Receiver maker and type	PolaRx5TR	PolaRx5TR	PolaRx5TR
Receiver serial number	3052427	3069829	3069591
1 PPS triger level / V	1	1	1
Antenna cable marker and type	LMR-400 type	HY 400 UF	HY 400 UF
Phase stabilized cable (Y/N)	Y	N	N
Cable length outside building / m	10	20	20
Antenna maker and type	LEICA AR20	TWIVP6000	TWIVP6000
Antenna serial number	22282006	33-685000-01-01	33-685000-01-01
Temperature if stabilized / °C	no		
Mesured delays / ns			
	Local	**Traveling**	
Delay from local UTC(k) to receiver 1 PPS_IN			
Delay from 1 PPS_IN to internal reference (see Annex 1)	Compensation disabled	Compensation disabled	Compensation disabled
Antenna cable delay	118.5 ns		
Splitter delay	na		
Additional cable delay	na		
Data used for the generation of CGGTTS files			
	Local	**Traveling**	
INT DLY (GPS) / ns	P1: 34.823 P2: 31.676	P1: 224.074 P2: 221.923	P1: 224.754 P2: 222.655
INT DLY (Galileo) / ns	E1: 36.933 E5a: 38.115	E1: 226.420 E5a: 225.980	E1: 227.241 E5a: 226.720
INT DLY (Beidou) / ns	B1c: 36.862 B2a: 37.538	B1c: 226.215 B2a: 225.411	B1c: 227.129 B2a: 226.152
CAB DLY / ns	118.5	0.0	0.0
REF DLY / ns	60.1	38.4	56.2
Coordinate reference frame	ITRF	ITRF	ITRF
Latitude or X / m	4627900.117	4627901.922	4627901.922
Longitude or Y / m	119894.648	119896.445	119896.445
Height or Z / m	4372941.440	4372939.828	4372939.828
General Information			
Rise time of local UTC pulse	0.5 ns		
Air conditioning (Y/N)	Y		
Set temperature value and uncertainty	22+/-1°C		
Set humidity value and uncertainty			

Cal Id: 1011-2025 Version / Date: 24/06/2025

BIPM Information sheet

Laboratory	LUX		
Date and hour beginning of measurements	24-02-2025 12:00 UTC		
Date and hour end measurements	03-03-2025 23:59 UTC		
Information on the system			
	Local	**Traveling**	
4-Character BIPM code	LU01	OP72	OP74
Receiver maker and type	PolaRx5TR	PolaRx5TR	PolaRx5TR
Receiver serial number	4701202	3069829	3069591
1 PPS triger level / V	1.0	1	1
Antenna cable marker and type	HUBER+SUHNER	HY 400 UF	HY 400 UF
Phase stabilized cable (Y/N)	N	N	N
Cable length outside building / m	< 2 m	20	20
Antenna maker and type	SEPCHOKE B3E6	TWIVP6000	TWIVP6000
Antenna serial number	5151	33-685000-01-01	33-685000-01-01
Temperature if stabilized / °C	na		
Mesured delays / ns			
	Local	**Traveling**	
Delay from local UTC(k) to receiver 1 PPS_IN	2.03		
Delay from 1 PPS_IN to internal reference (see Annex 1)	34.512, Compensation disabled	Compensation disabled	Compensation disabled
Antenna cable delay	117.4		
Splitter delay	na		
Additional cable delay	na		
Data used for the generation of CGGTTS files			
	Local	**Traveling**	
INT DLY (GPS) / ns	P1: 28.170 P2: 25.062	P1: 224.074 P2: 221.923	P1: 224.754 P2: 222.655
INT DLY (Galileo) / ns	E1: 30.636 E5a: 30.974	E1: 226.420 E5a: 225.980	E1: 227.241 E5a: 226.720
INT DLY (Beidou) / ns	B1c: B2a:	B1c: B2a:	B1c: B2a:
CAB DLY / ns	117.4	0.0	0.0
REF DLY / ns	36.6	50.2	68.2
Coordinate reference frame	ITRF	ITRF	ITRF
Latitude or X / m	4127838.687	4127842.970	4127842.970
Longitude or Y / m	430296.280	430283.031	430283.031
Height or Z / m	4827426.255	4827423.826	4827423.826
General Information			
Rise time of local UTC pulse	350 ps		
Air conditioning (Y/N)	Y		
Set temperature value and uncertainty	23±3 °C		
Set humidity value and uncertainty	< 80 %Hr		

Cal Id: 1011-2025 Version / Date: 24/06/2025

BIPM Information sheet

Laboratory	LUX		
Date and hour beginning of measurements	24-02-2025 12:00 UTC		
Date and hour end measurements	03-03-2025 23:59 UTC		
Information on the system			
	Local	**Traveling**	
4-Character BIPM code	LU02	OP72	OP74
Receiver maker and type	PolaRx5TR	PolaRx5TR	PolaRx5TR
Receiver serial number	4701382	3069829	3069591
1 PPS triger level / V	1.0	1	1
Antenna cable marker and type	HUBER+SUHNER	HY 400 UF	HY 400 UF
Phase stabilized cable (Y/N)	N	N	N
Cable length outside building / m	< 2 m	20	20
Antenna maker and type	SEPCHOKE B3E6	TWIVP6000	TWIVP6000
Antenna serial number	5668	33-685000-01-01	33-685000-01-01
Temperature if stabilized / °C	na		
Mesured delays / ns			
	Local	**Traveling**	
Delay from local UTC(k) to receiver 1 PPS_IN	1.53		
Delay from 1 PPS_IN to internal reference (see Annex 1)	37.03, Compensation disabled	Compensation disabled	Compensation disabled
Antenna cable delay	160.63		
Splitter delay	na		
Additional cable delay	na		
Data used for the generation of CGGTTS files			
	Local	**Traveling**	
INT DLY (GPS) / ns	P1: 30.550 P2: 27.694	P1: 224.074 P2: 221.923	P1: 224.754 P2: 222.655
INT DLY (Galileo) / ns	E1: 32.812 E5a: 31.495	E1: 226.420 E5a: 225.980	E1: 227.241 E5a: 226.720
INT DLY (Beidou) / ns	B1c: 32.440 B2a: 30.972	B1c: 226.215 B2a: 225.411	B1c: 227.129 B2a: 226.152
CAB DLY / ns	160.6	0.0	0.0
REF DLY / ns	38.6	50.2	68.2
Coordinate reference frame	ITRF	ITRF	ITRF
Latitude or X / m	4127842.231	4127842.970	4127842.970
Longitude or Y / m	430283.302	430283.031	430283.031
Height or Z / m	4827424.428	4827423.826	4827423.826
General Information			
Rise time of local UTC pulse	350 ps		
Air conditioning (Y/N)	Y		
Set temperature value and uncertainty	23±3 °C		
Set humidity value and uncertainty	< 80 %Hr		

B Annex B: Plots of raw data and TDEV analysis for GPS and Galileo.

B.1 GPS calibration.

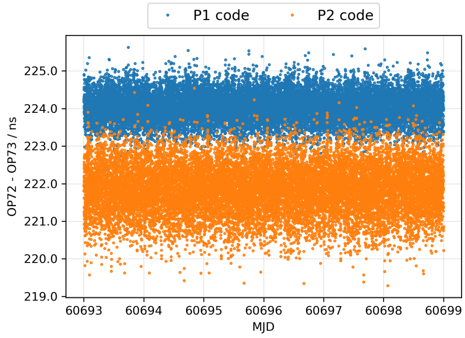

(a) P-code phase differences

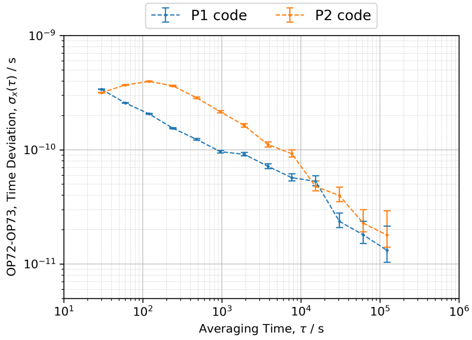

(b) TDEV of P-code delays

Figure 8: Relative calibration of OP72 with respect to OP73

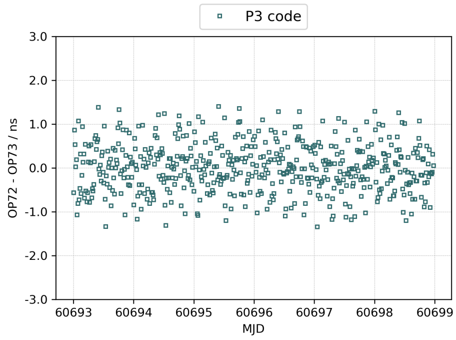

(a) P3 CV after calibration

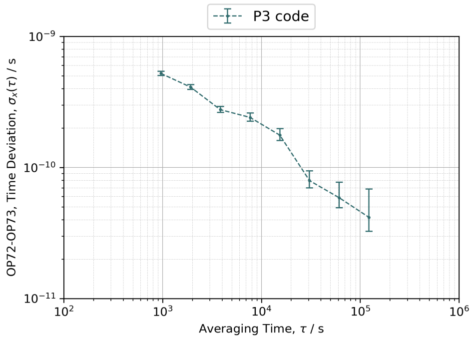

(b) TDEV of P3 CV

Figure 9: P3 CV time difference OP72 with respect to OP73

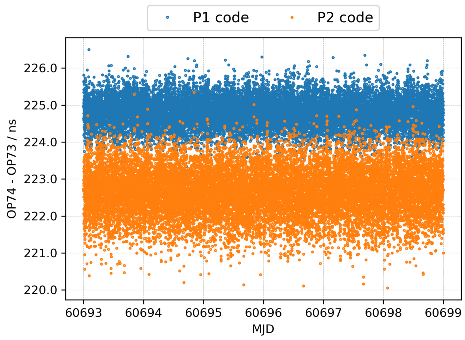

(a) P-code phase differences

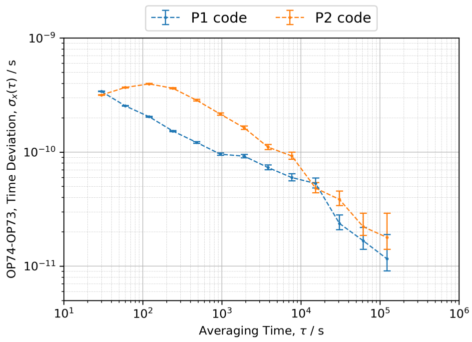

(b) TDEV of P-code delays

Figure 10: Relative calibration of OP74 with respect to OP73

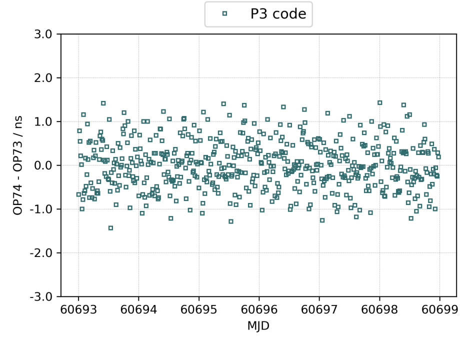

(a) P3 CV after calibration

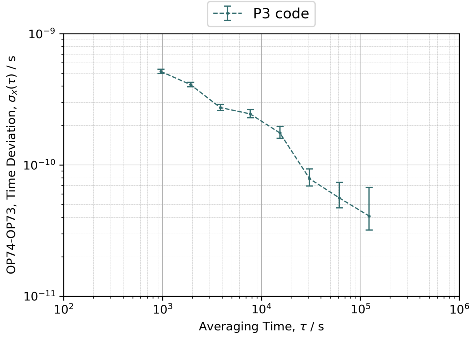

(b) TDEV of P3 CV

Figure 11: P3 CV time difference OP74 with respect to OP73

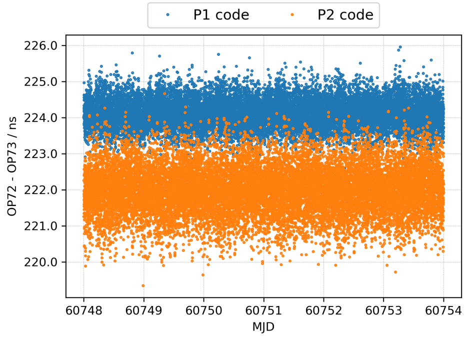

(a) P-code phase differences

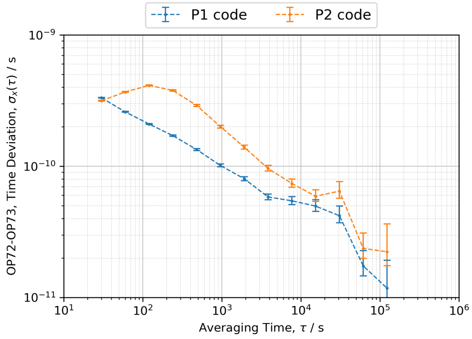

(b) TDEV of P-code delays

Figure 12: Relative calibration of OP72 with respect to OP73

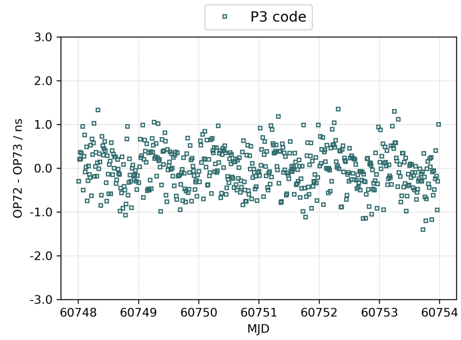

(a) P3 CV after calibration

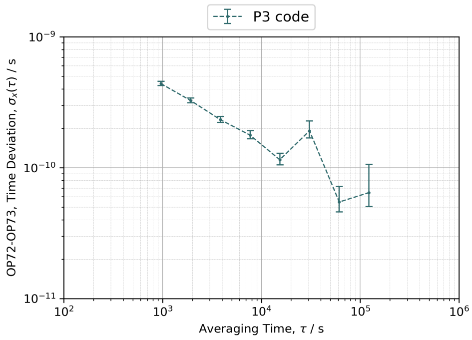

(b) TDEV of P3 CV

Figure 13: P3 CV time difference OP72 with respect to OP73

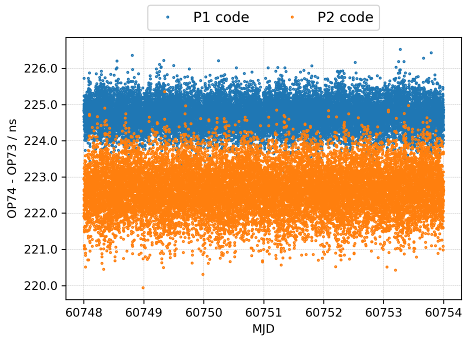

(a) P-code phase differences

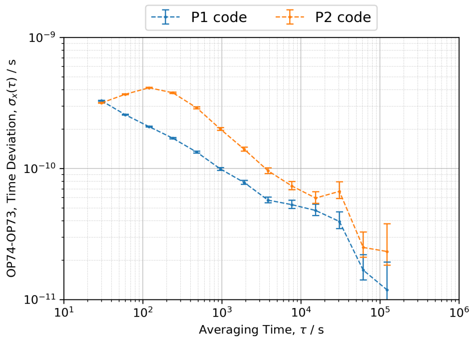

(b) TDEV of P-code delays

Figure 14: Relative calibration of OP74 with respect to OP73

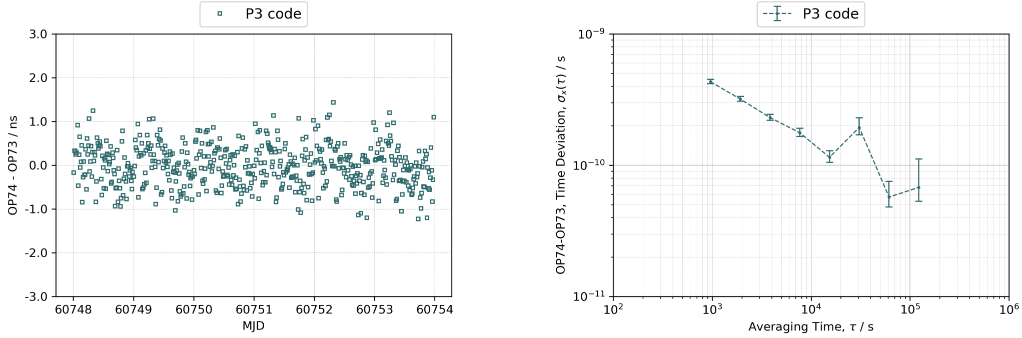

(a) P3 CV after calibration

(b) TDEV of P3 CV

Figure 15: P3 CV time difference OP74 with respect to OP73

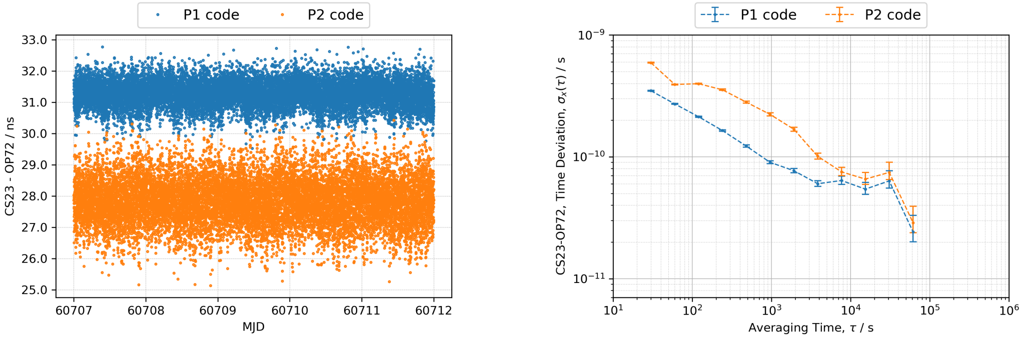

(a) P-code phase differences

(b) TDEV of P-code delays

Figure 16: Relative calibration of CS23 with respect to OP72

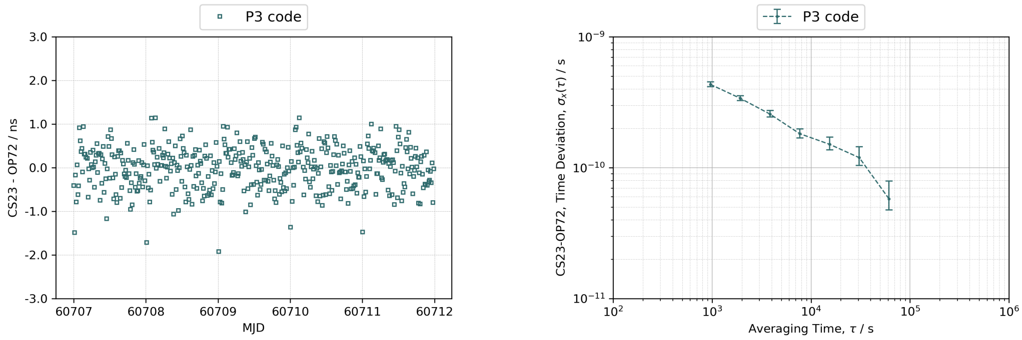

(a) P3 CV after calibration

(b) TDEV of P3 CV

Figure 17: P3 CV time difference CS23 with respect to OP72

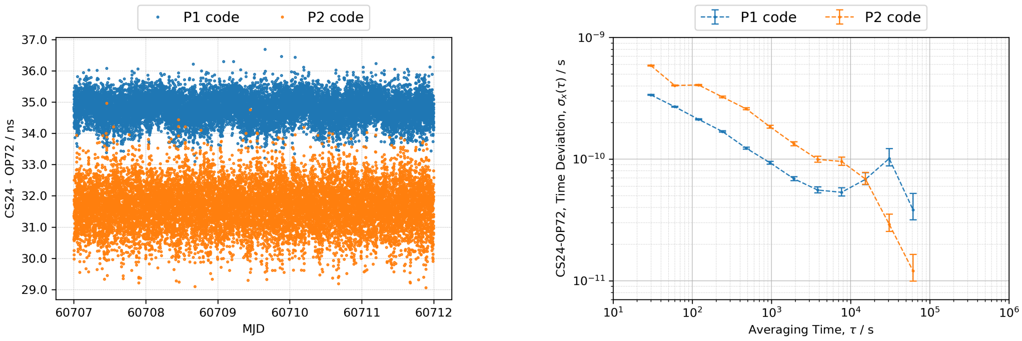

(a) P-code phase differences

(b) TDEV of P-code delays

Figure 18: Relative calibration of CS24 with respect to OP72

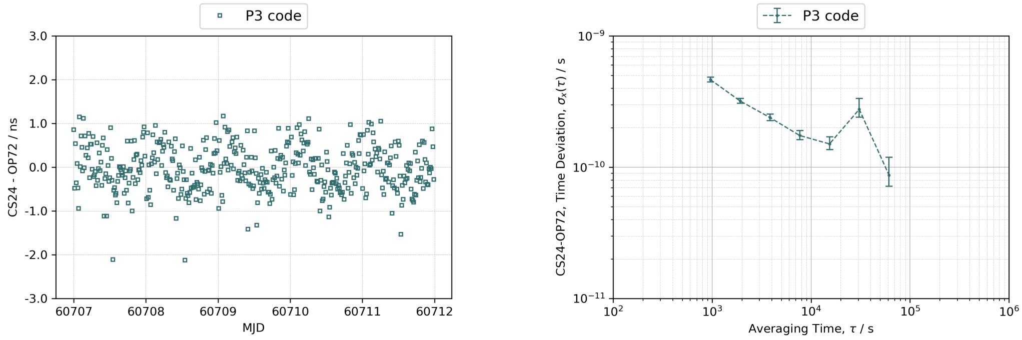

(a) P3 CV after calibration

(b) TDEV of P3 CV

Figure 19: P3 CV time difference CS24 with respect to OP72

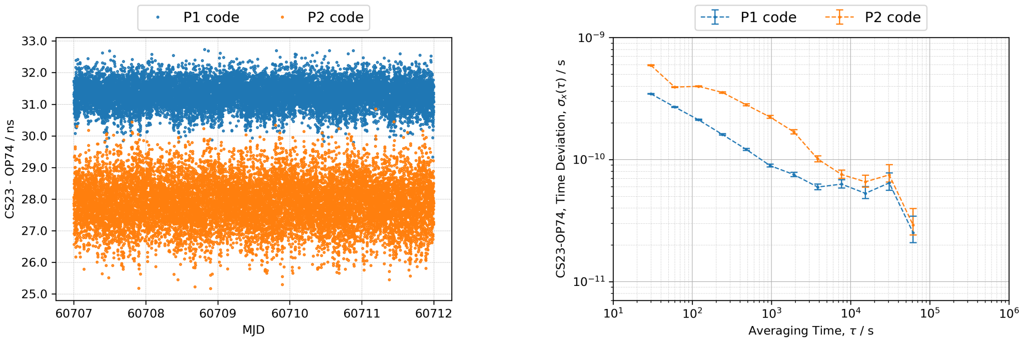

(a) P-code phase differences

(b) TDEV of P-code delays

Figure 20: Relative calibration of CS23 with respect to OP74

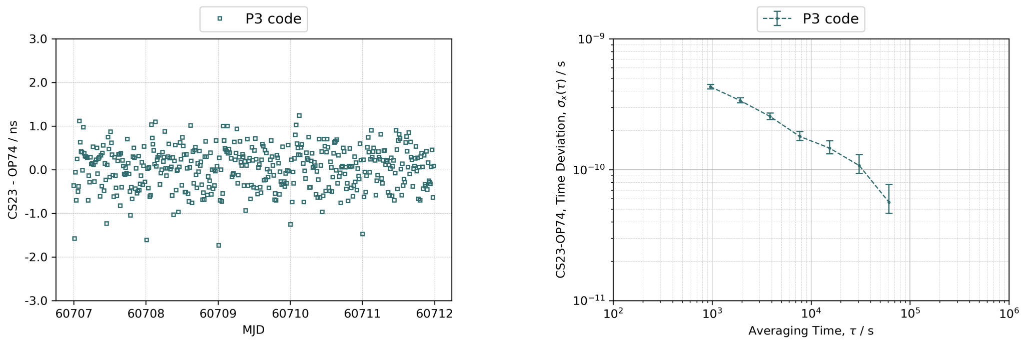

(a) P3 CV after calibration

(b) TDEV of P3 CV

Figure 21: P3 CV time difference CS23 with respect to OP74

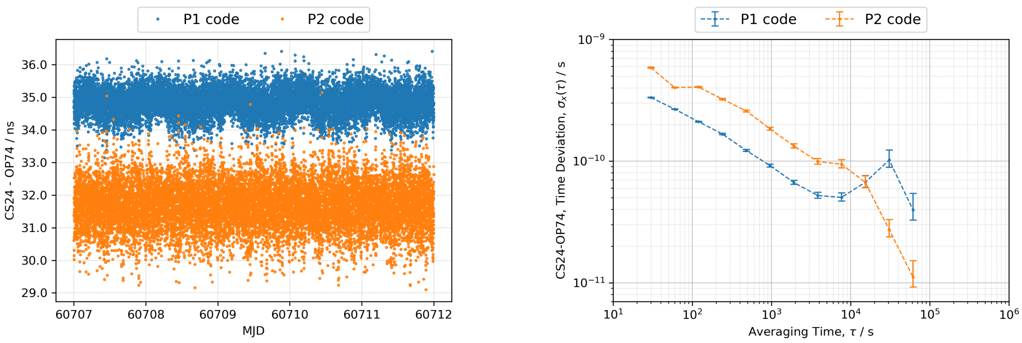

(a) P-code phase differences

(b) TDEV of P-code delays

Figure 22: Relative calibration of CS24 with respect to OP74

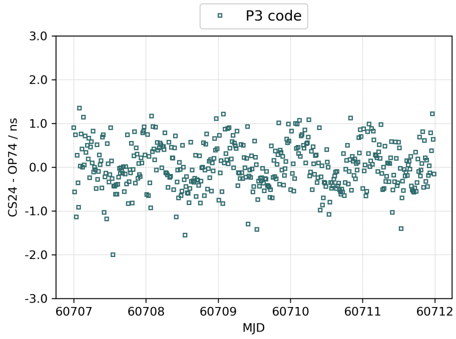

(a) P3 CV after calibration

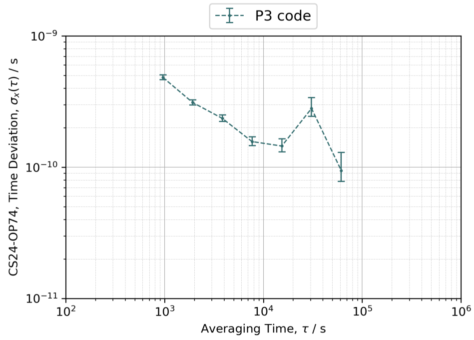

(b) TDEV of P3 CV

Figure 23: P3 CV time difference CS24 with respect to OP74

(a) P-code phase differences

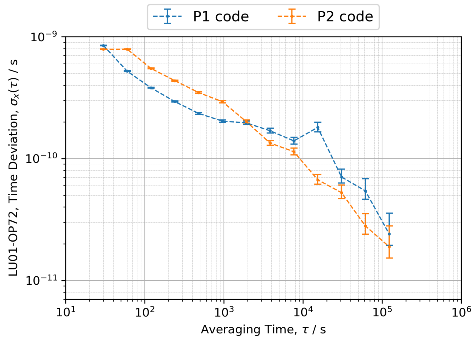

(b) TDEV of P-code delays

Figure 24: Relative calibration of LU01 with respect to OP72

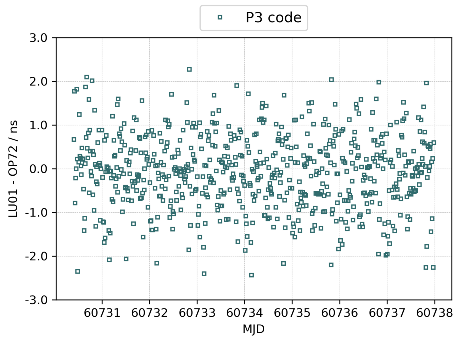

(a) P3 CV after calibration

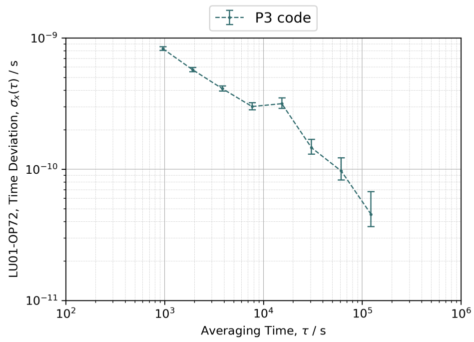

(b) TDEV of P3 CV

Figure 25: P3 CV time difference LU01 with respect to OP72

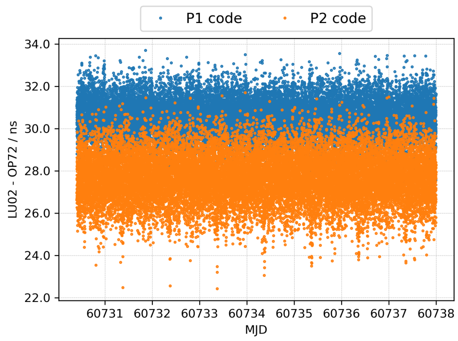

(a) P-code phase differences

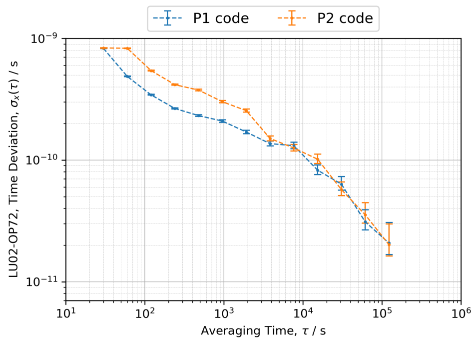

(b) TDEV of P-code delays

Figure 26: Relative calibration of LU02 with respect to OP72

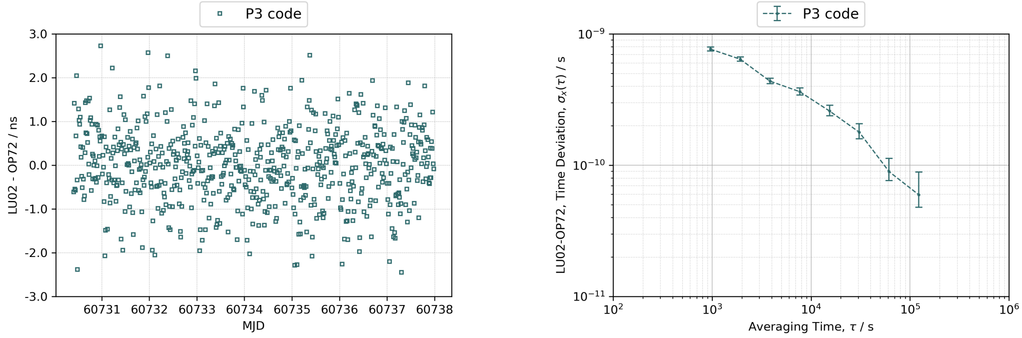

(a) P3 CV after calibration

(b) TDEV of P3 CV

Figure 27: P3 CV time difference LU02 with respect to OP72

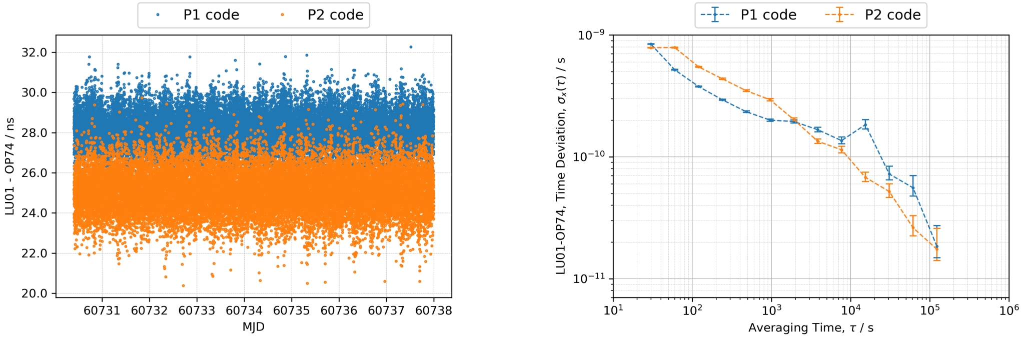

(a) P-code phase differences

(b) TDEV of P-code delays

Figure 28: Relative calibration of LU01 with respect to OP74

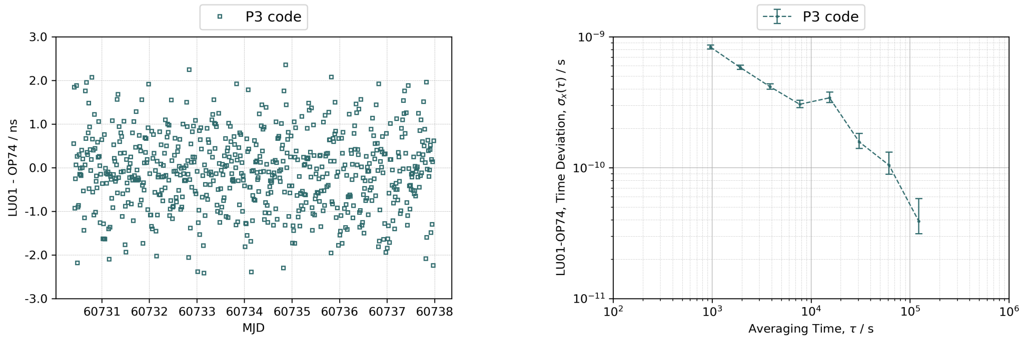

(a) P3 CV after calibration

(b) TDEV of P3 CV

Figure 29: P3 CV time difference LU01 with respect to OP74

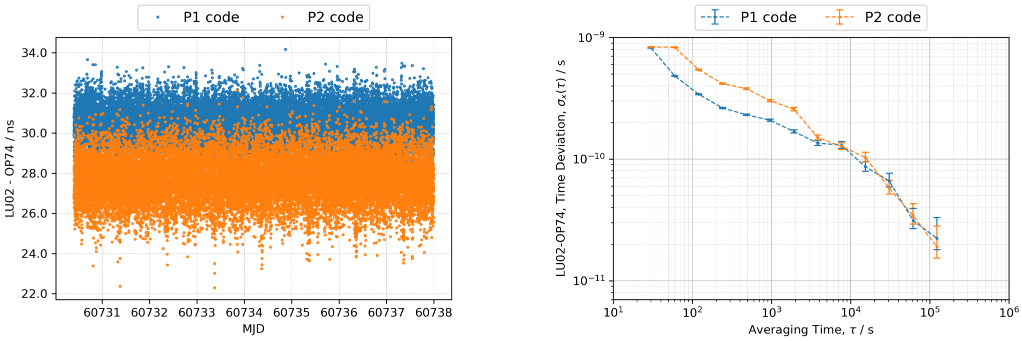

(a) P-code phase differences

(b) TDEV of P-code delays

Figure 30: Relative calibration of LU02 with respect to OP74

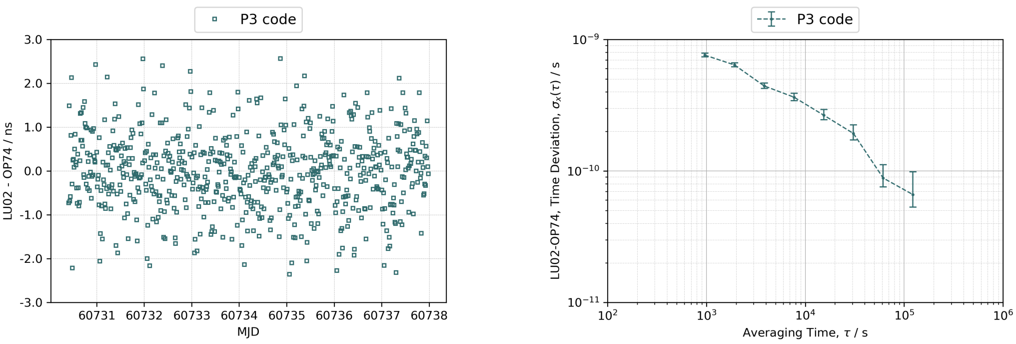

(a) P3 CV after calibration

(b) TDEV of P3 CV

Figure 31: P3 CV time difference LU02 with respect to OP74

B.2 Galileo calibration.

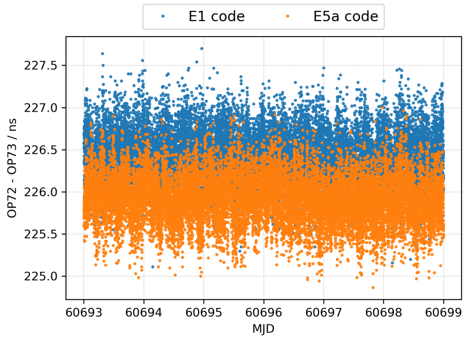

(a) E-code phase differences

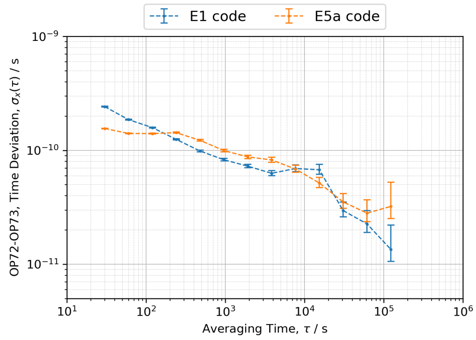

(b) TDEV of E-code delays

Figure 32: Relative calibration of OP72 with respect to OP73

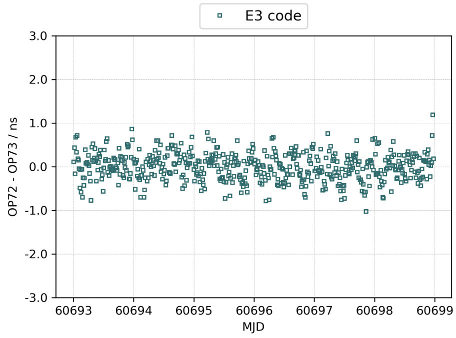

(a) E3 CV after calibration

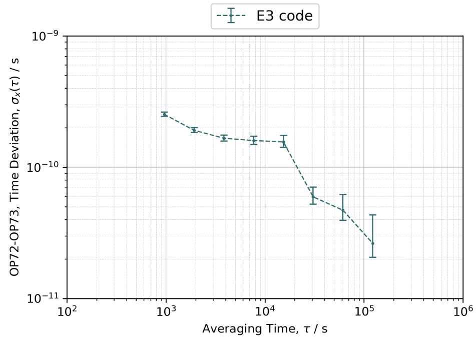

(b) TDEV of E3 CV

Figure 33: E3 CV time difference OP72 with respect to OP73

(a) E-code phase differences

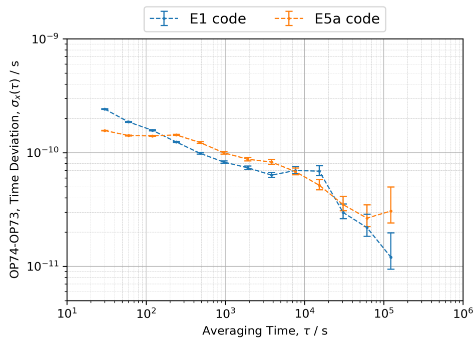

(b) TDEV of E-code delays

Figure 34: Relative calibration of OP74 with respect to OP73

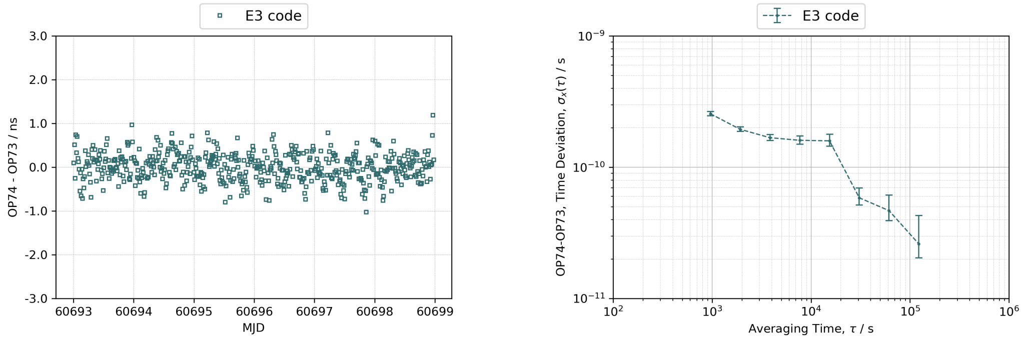

(a) E3 CV after calibration (b) TDEV of E3 CV

Figure 35: E3 CV time difference OP74 with respect to OP73

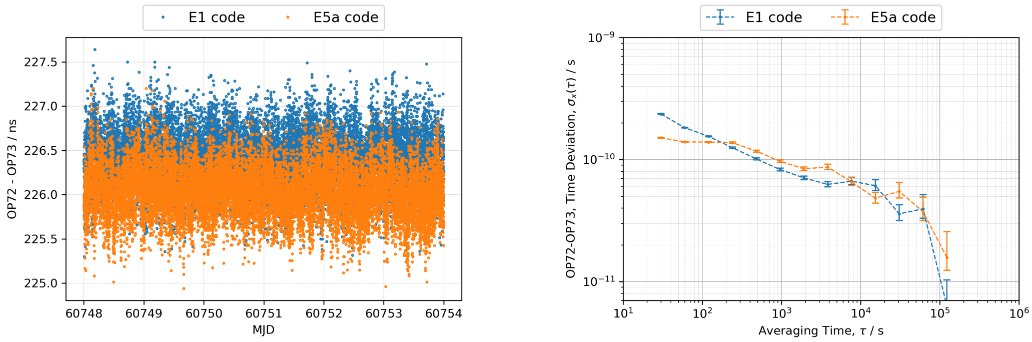

(a) E-code phase differences (b) TDEV of E-code delays

Figure 36: Relative calibration of OP72 with respect to OP73

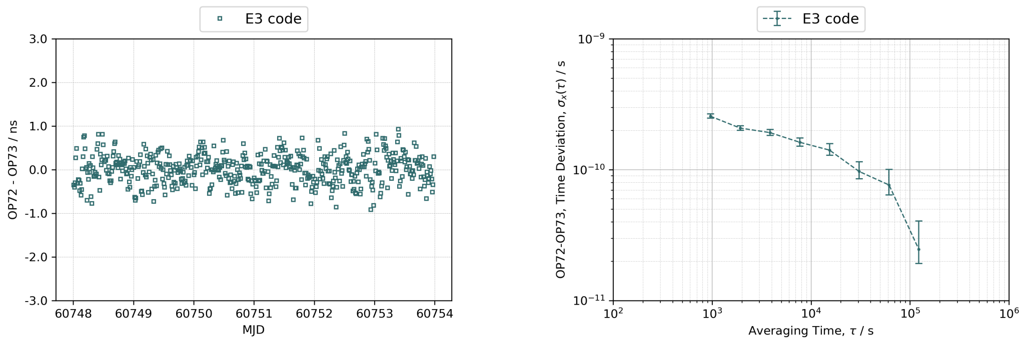

(a) E3 CV after calibration (b) TDEV of E3 CV

Figure 37: E3 CV time difference OP72 with respect to OP73

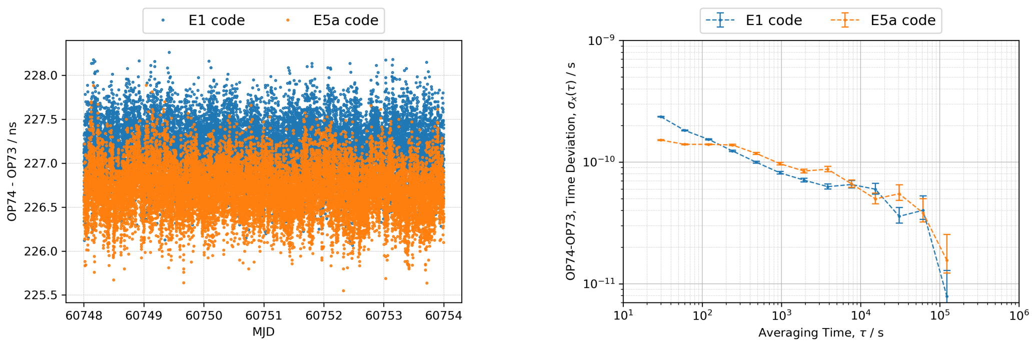

(a) E-code phase differences (b) TDEV of E-code delays

Figure 38: Relative calibration of OP74 with respect to OP73

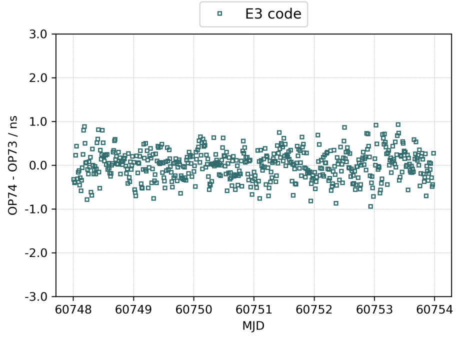

(a) E3 CV after calibration

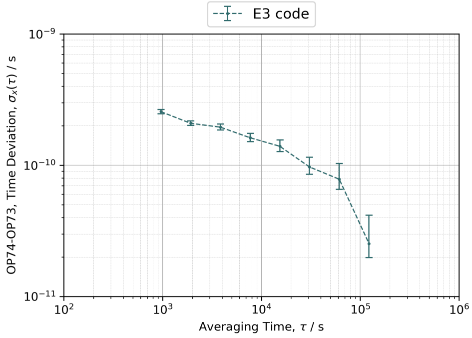

(b) TDEV of E3 CV

Figure 39: E3 CV time difference OP74 with respect to OP73

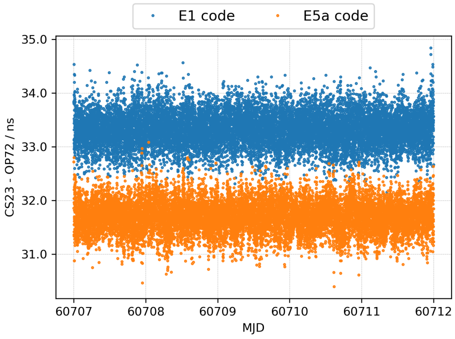

(a) E-code phase differences

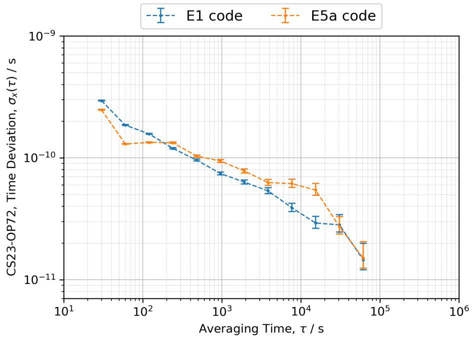

(b) TDEV of E-code delays

Figure 40: Relative calibration of CS23 with respect to OP72

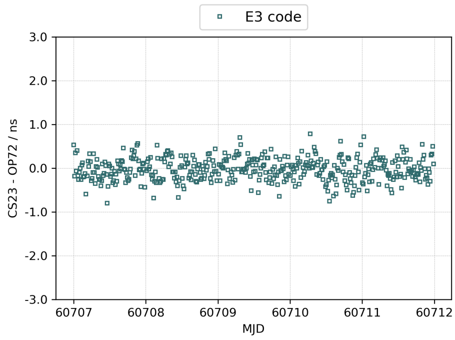

(a) E3 CV after calibration

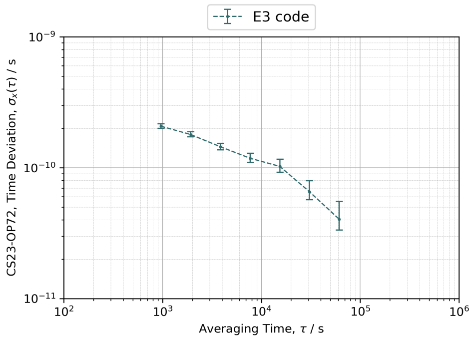

(b) TDEV of E3 CV

Figure 41: E3 CV time difference CS23 with respect to OP72

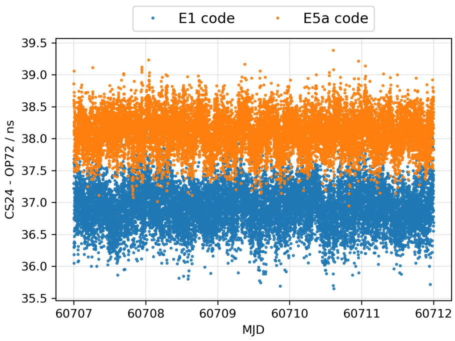

(a) E-code phase differences

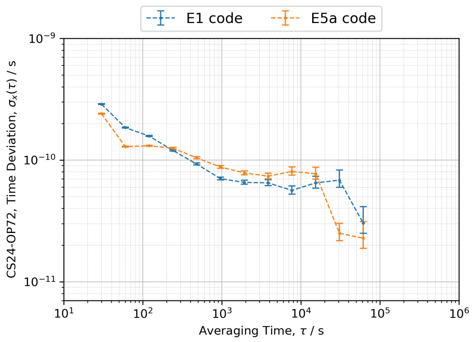

(b) TDEV of E-code delays

Figure 42: Relative calibration of CS24 with respect to OP72

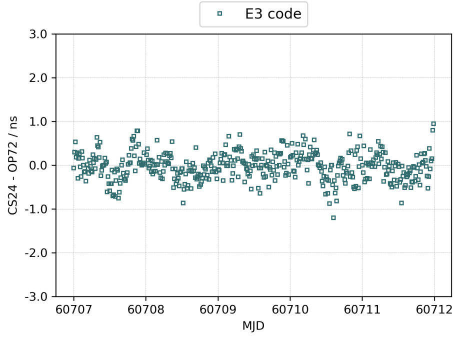

(a) E3 CV after calibration

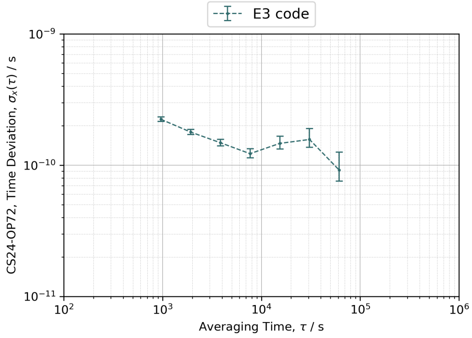

(b) TDEV of E3 CV

Figure 43: E3 CV time difference CS24 with respect to OP72

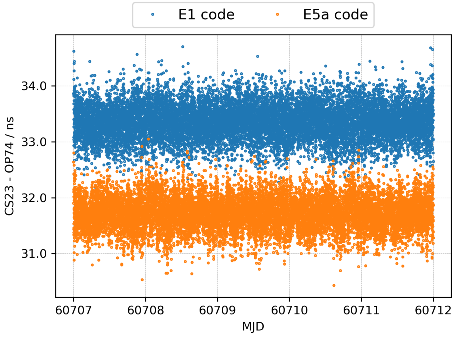

(a) E-code phase differences

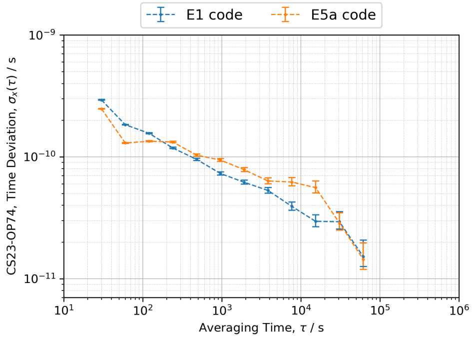

(b) TDEV of E-code delays

Figure 44: Relative calibration of CS23 with respect to OP74

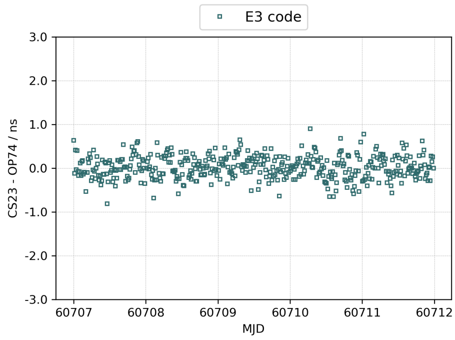

(a) E3 CV after calibration

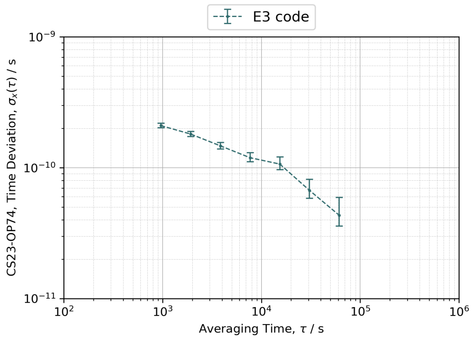

(b) TDEV of E3 CV

Figure 45: E3 CV time difference CS23 with respect to OP74

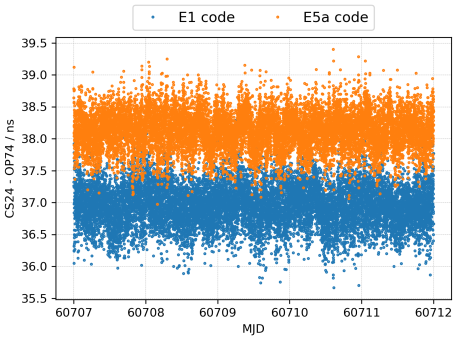

(a) E-code phase differences

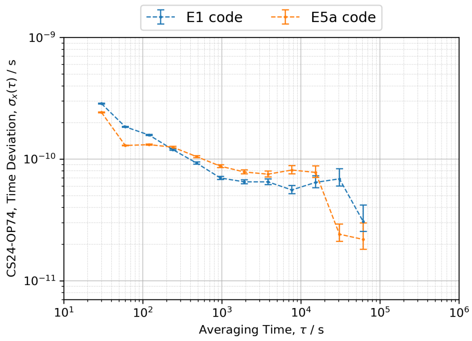

(b) TDEV of E-code delays

Figure 46: Relative calibration of CS24 with respect to OP74

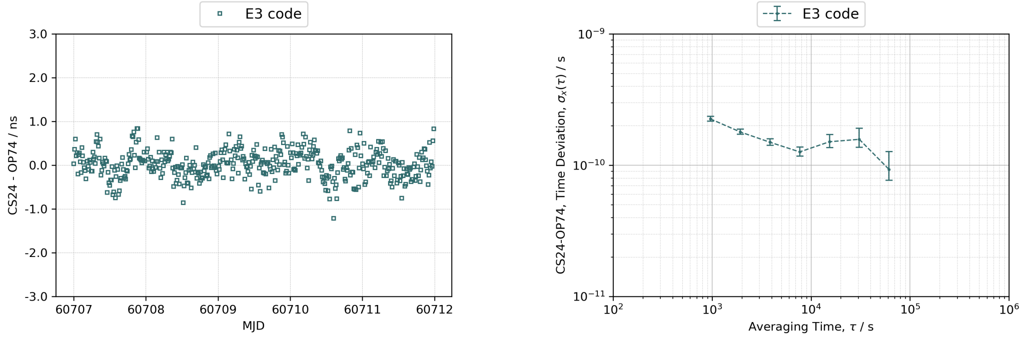

(a) E3 CV after calibration (b) TDEV of E3 CV

Figure 47: E3 CV time difference CS24 with respect to OP74

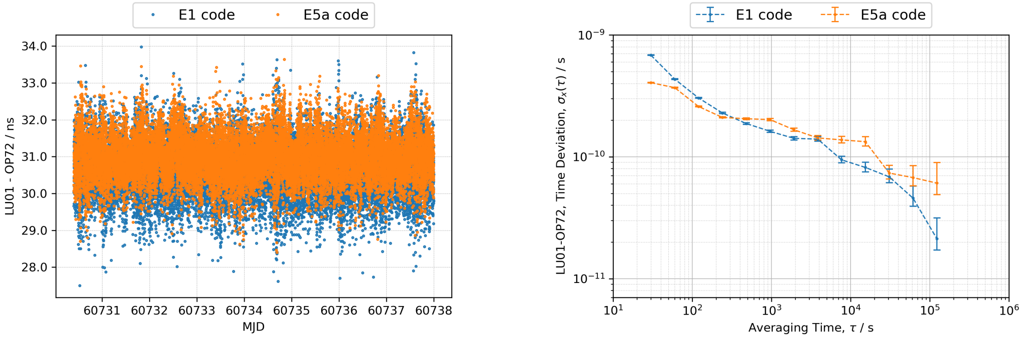

(a) E-code phase differences (b) TDEV of E-code delays

Figure 48: Relative calibration of LU01 with respect to OP72

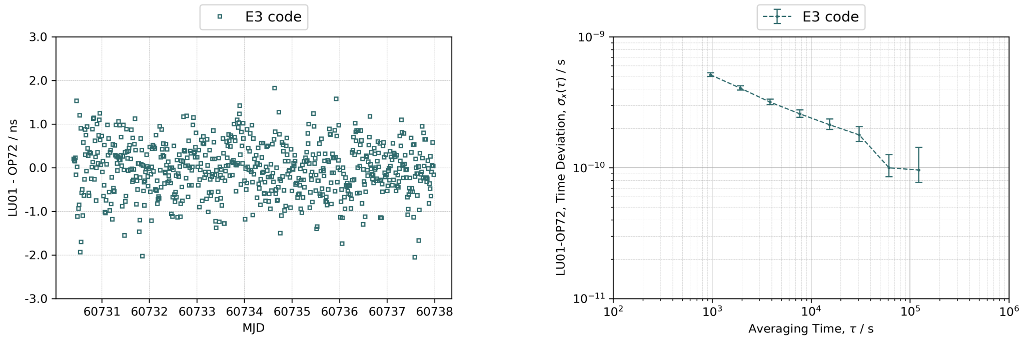

(a) E3 CV after calibration (b) TDEV of E3 CV

Figure 49: E3 CV time difference LU01 with respect to OP72

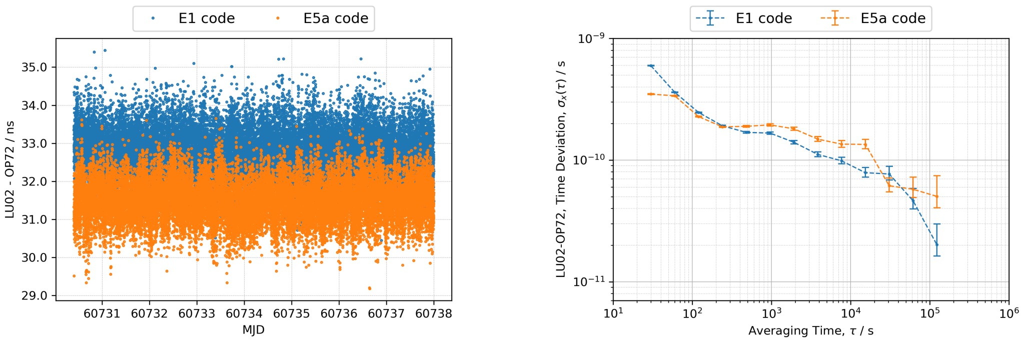

(a) E-code phase differences (b) TDEV of E-code delays

Figure 50: Relative calibration of LU02 with respect to OP72

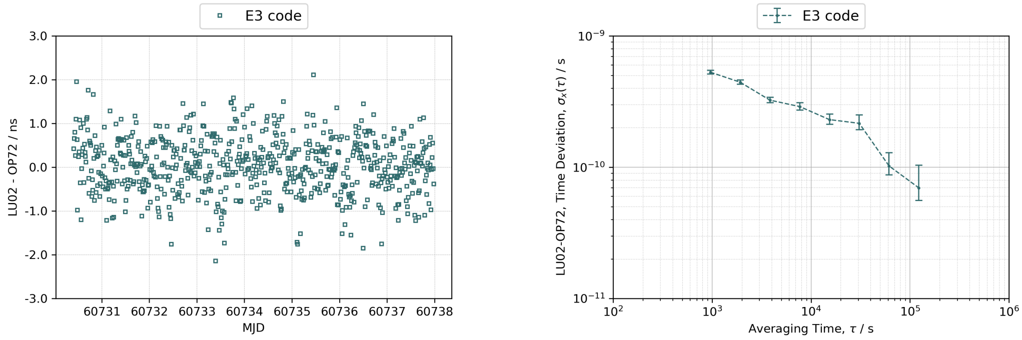

(a) E3 CV after calibration

(b) TDEV of E3 CV

Figure 51: E3 CV time difference LU02 with respect to OP72

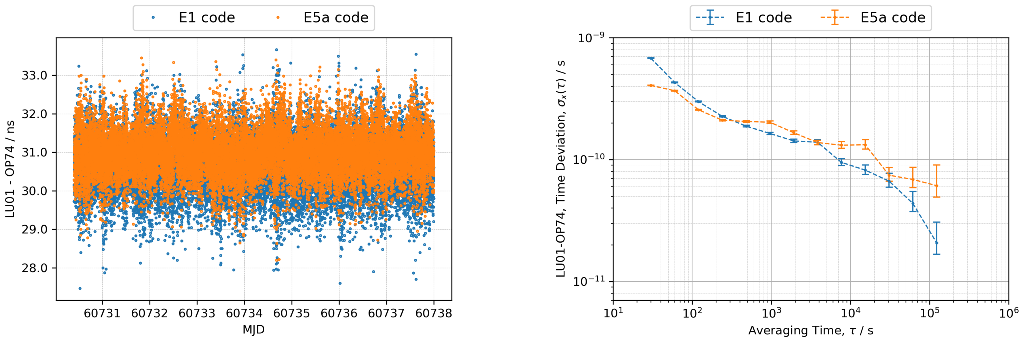

(a) E-code phase differences

(b) TDEV of E-code delays

Figure 52: Relative calibration of LU01 with respect to OP74

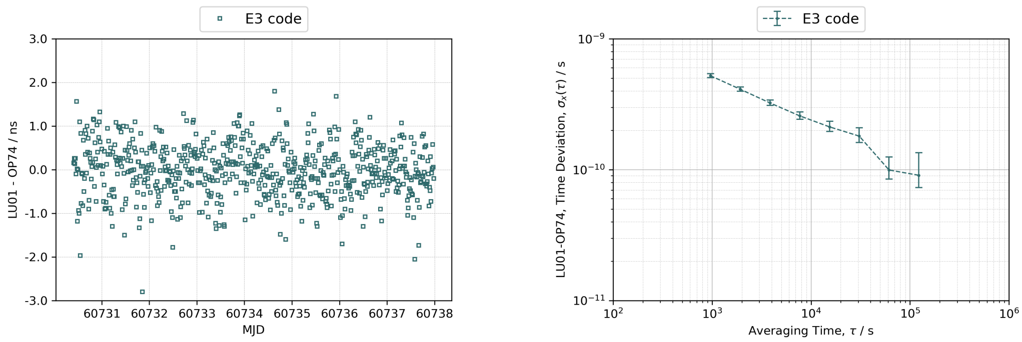

(a) E3 CV after calibration

(b) TDEV of E3 CV

Figure 53: E3 CV time difference LU01 with respect to OP74

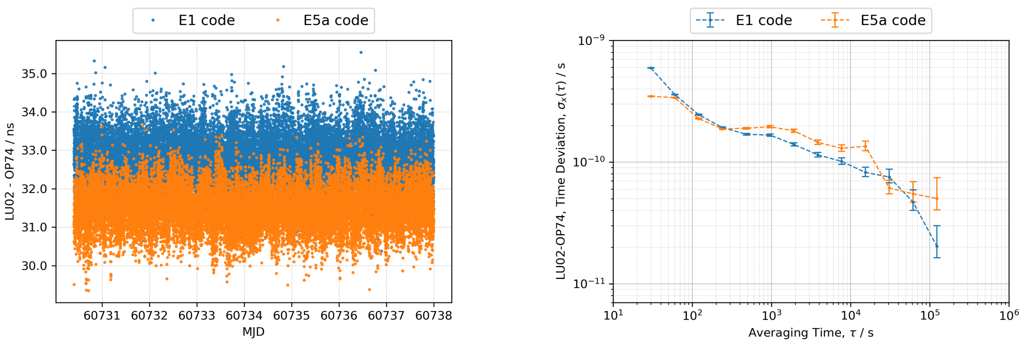

(a) E-code phase differences

(b) TDEV of E-code delays

Figure 54: Relative calibration of LU02 with respect to OP74

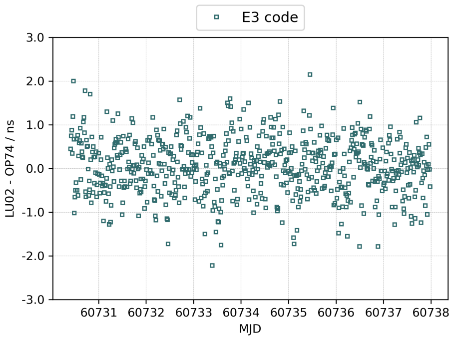

(a) E3 CV after calibration

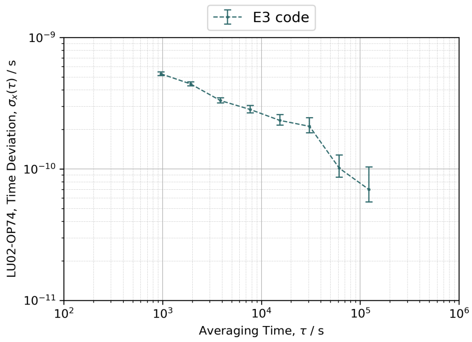

(b) TDEV of E3 CV

Figure 55: E3 CV time difference LU02 with respect to OP74

B.3 Beidou calibration.

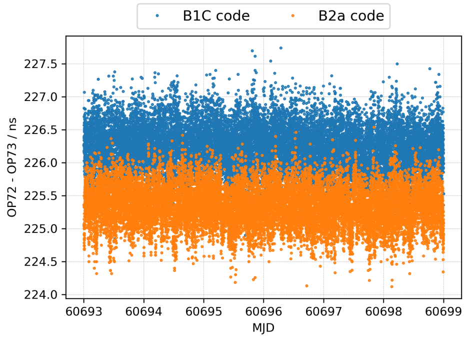

(a) B-code phase differences

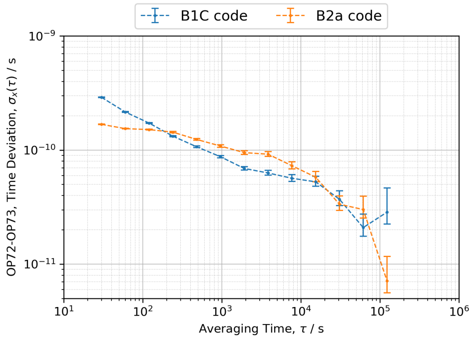

(b) TDEV of B-code delays

Figure 56: Relative calibration of OP72 with respect to OP73

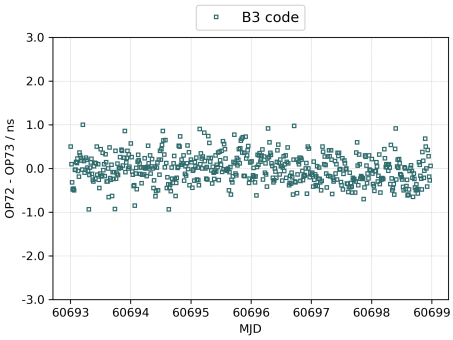

(a) B3 CV after calibration

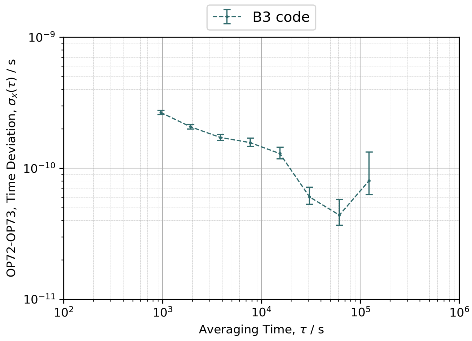

(b) TDEV of B3 CV

Figure 57: B3 CV time difference OP72 with respect to OP73

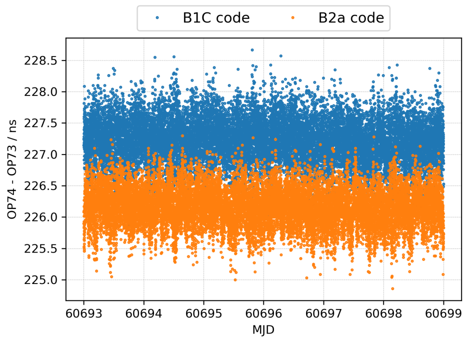

(a) B-code phase differences

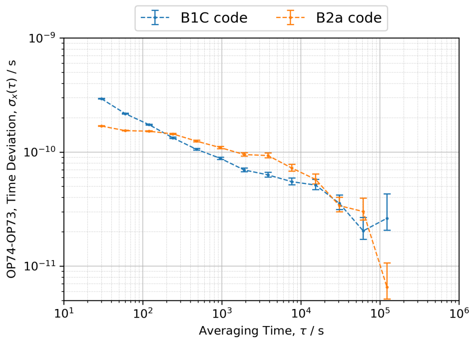

(b) TDEV of B-code delays

Figure 58: Relative calibration of OP74 with respect to OP73

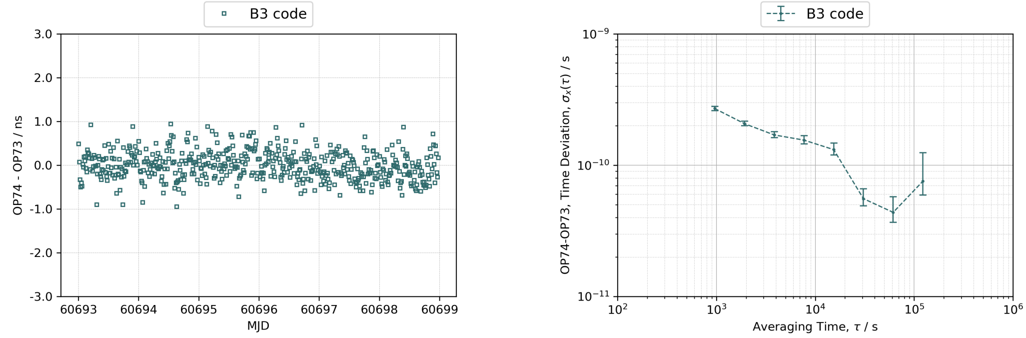

(a) B3 CV after calibration (b) TDEV of B3 CV

Figure 59: B3 CV time difference OP74 with respect to OP73

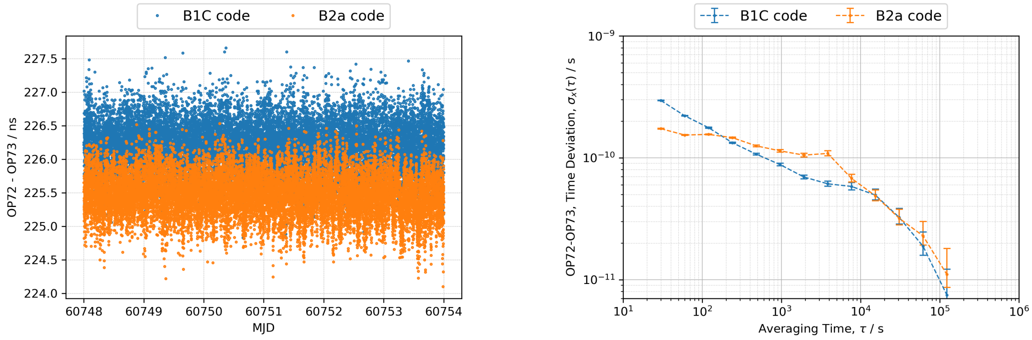

(a) B-code phase differences (b) TDEV of B-code delays

Figure 60: Relative calibration of OP72 with respect to OP73

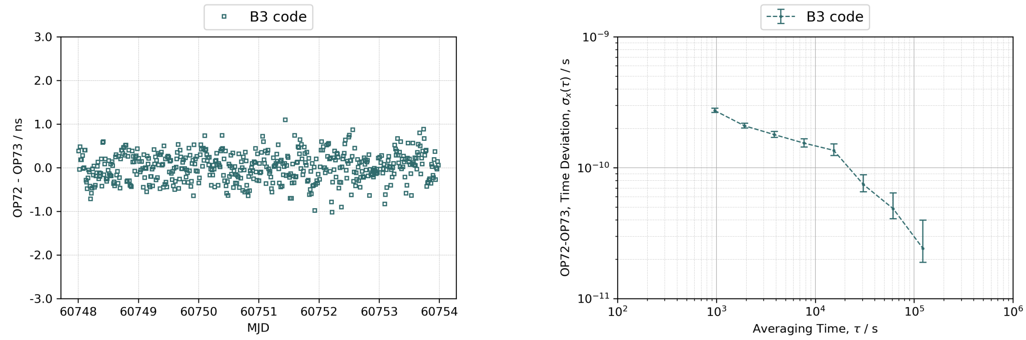

(a) B3 CV after calibration (b) TDEV of B3 CV

Figure 61: B3 CV time difference OP72 with respect to OP73

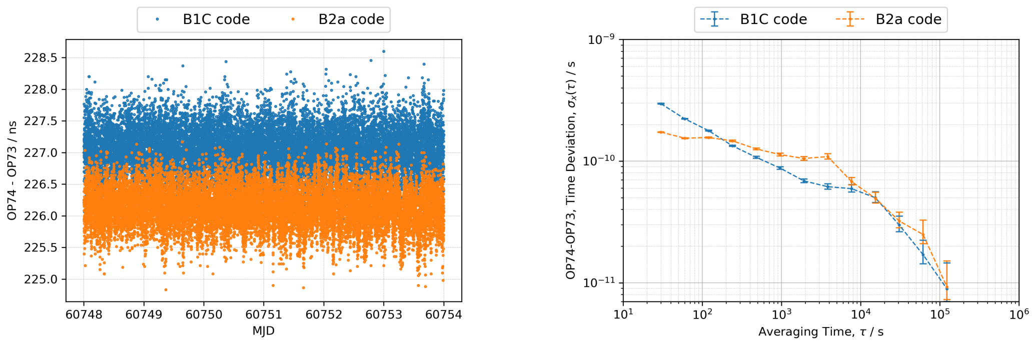

(a) B-code phase differences (b) TDEV of B-code delays

Figure 62: Relative calibration of OP74 with respect to OP73

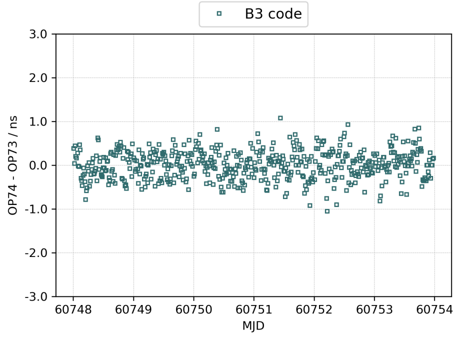

(a) B3 CV after calibration

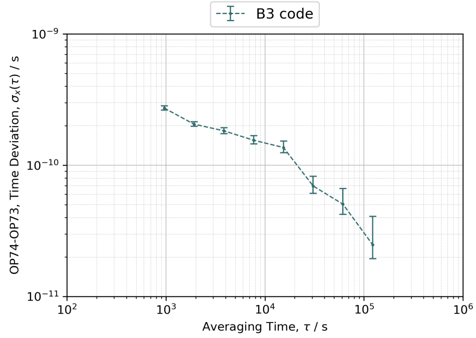

(b) TDEV of B3 CV

Figure 63: B3 CV time difference OP74 with respect to OP73

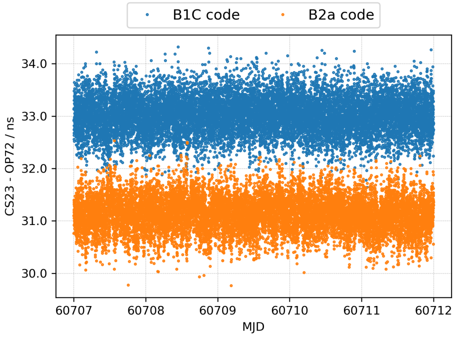

(a) B-code phase differences

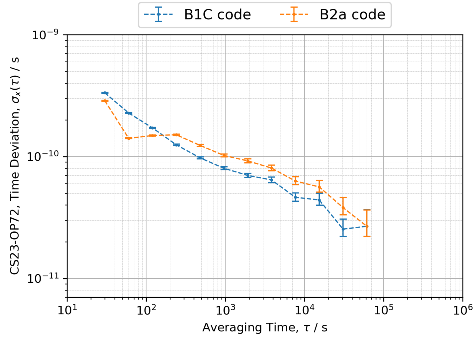

(b) TDEV of B-code delays

Figure 64: Relative calibration of CS23 with respect to OP72

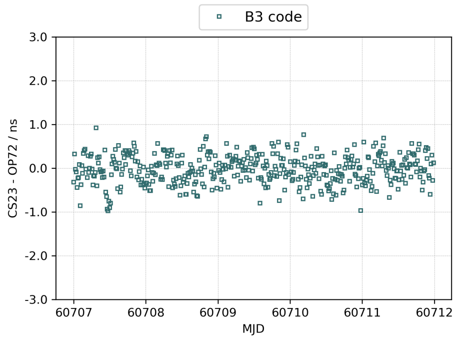

(a) B3 CV after calibration

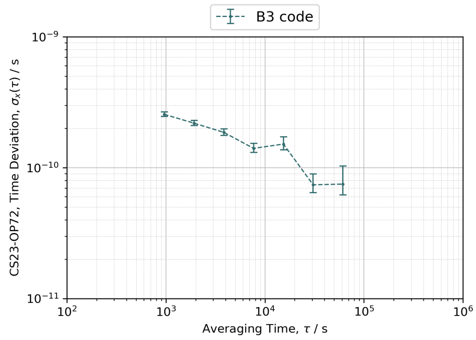

(b) TDEV of B3 CV

Figure 65: B3 CV time difference CS23 with respect to OP72

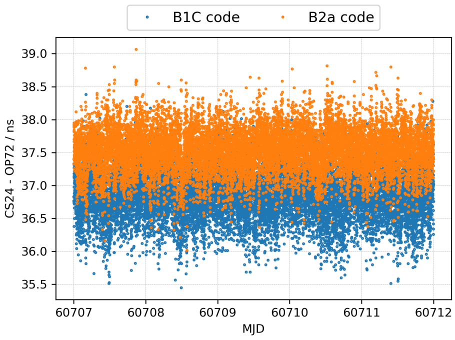

(a) B-code phase differences

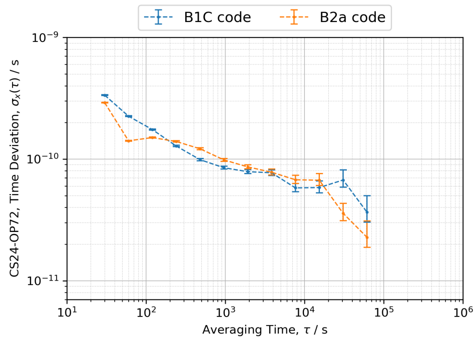

(b) TDEV of B-code delays

Figure 66: Relative calibration of CS24 with respect to OP72

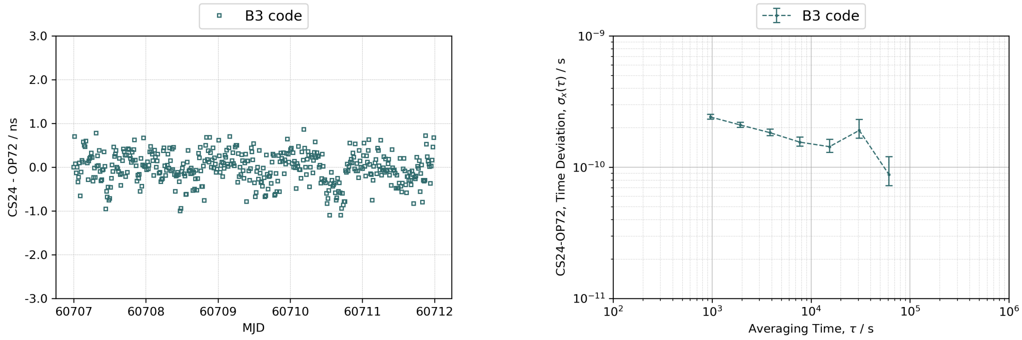

(a) B3 CV after calibration (b) TDEV of B3 CV

Figure 67: B3 CV time difference CS24 with respect to OP72

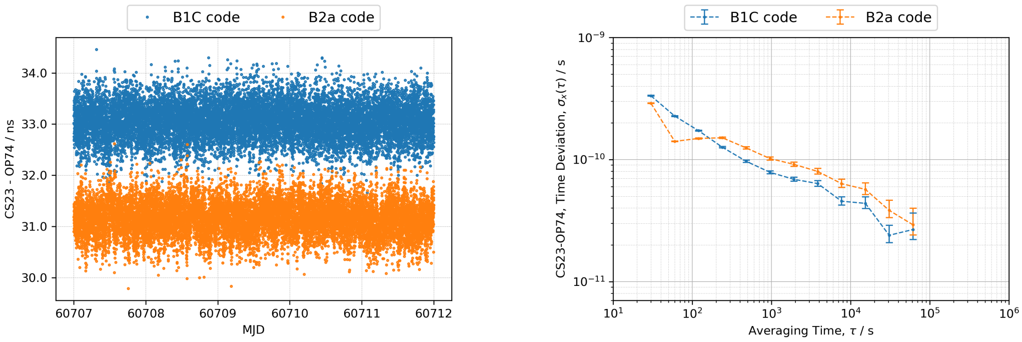

(a) B-code phase differences (b) TDEV of B-code delays

Figure 68: Relative calibration of CS23 with respect to OP74

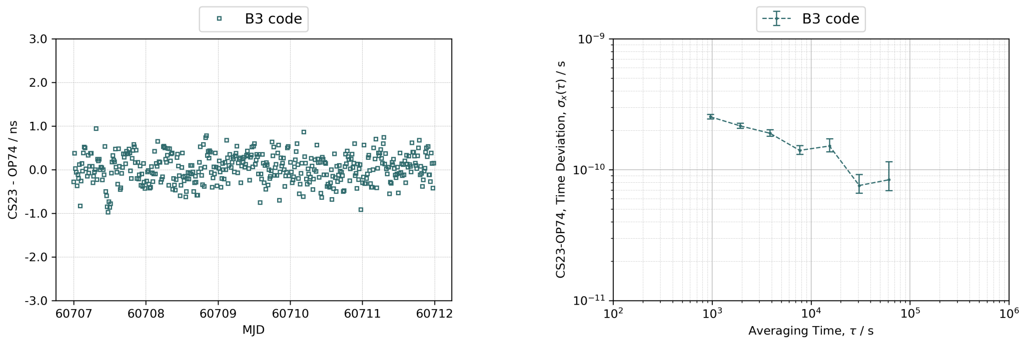

(a) B3 CV after calibration (b) TDEV of B3 CV

Figure 69: B3 CV time difference CS23 with respect to OP74

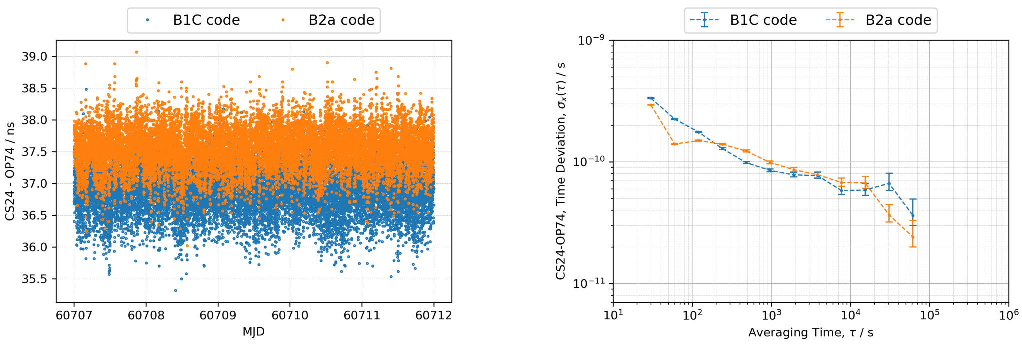

(a) B-code phase differences (b) TDEV of B-code delays

Figure 70: Relative calibration of CS24 with respect to OP74

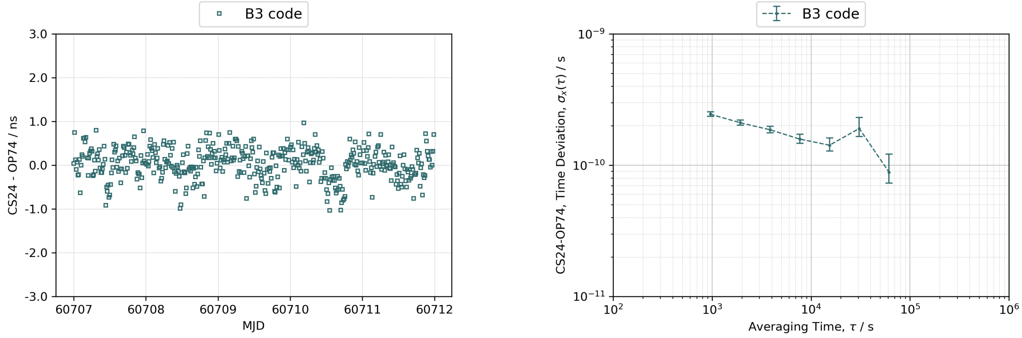

(a) B3 CV after calibration

(b) TDEV of B3 CV

Figure 71: B3 CV time difference CS24 with respect to OP74

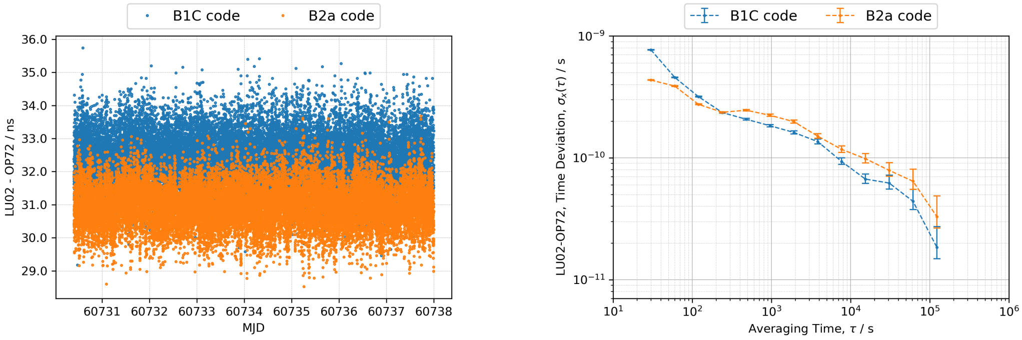

(a) B-code phase differences

(b) TDEV of B-code delays

Figure 72: Relative calibration of LU02 with respect to OP72

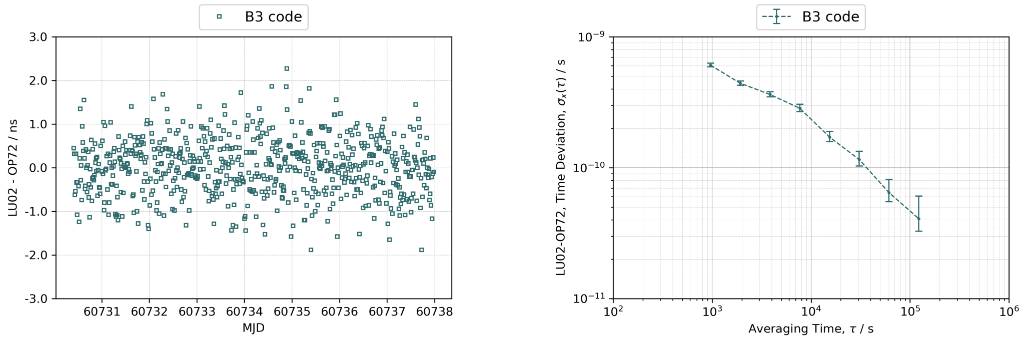

(a) B3 CV after calibration

(b) TDEV of B3 CV

Figure 73: B3 CV time difference LU02 with respect to OP72

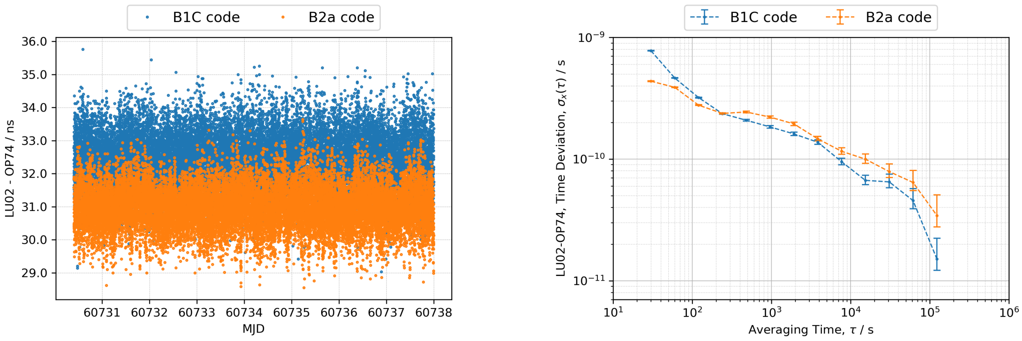

(a) B-code phase differences

(b) TDEV of B-code delays

Figure 74: Relative calibration of LU02 with respect to OP74

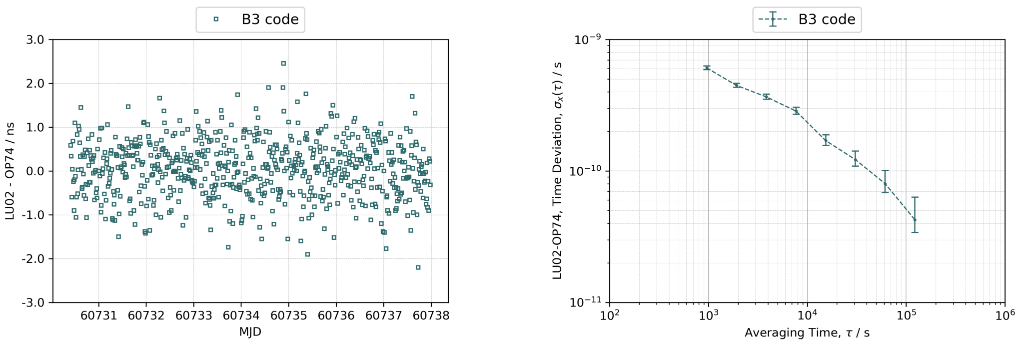

(a) B3 CV after calibration (b) TDEV of B3 CV

Figure 75: B3 CV time difference LU02 with respect to OP74

C Annex C: Uncertainty budget terms.

This section describes the uncertainty budget terms in the case of a calibration with a traveling equipment, including opening and closure measurement at OP.

C.1 Type A uncertainty.

The statistical uncertainty u_a(A-B) for the comparison between two GNSS stations A and B and for each GNSS code is evaluated by computing the upper limit of the error bar of the TDEV at 1 d when possible, or otherwise the upper limit of the last error bar available. The sampling periods of computed calibrated offset usually lead to TDEV data available for 61 440 s and 122 880 s averaging periods. The computed u_a is obtained by a linear interpolation between consecutive TDEV data at an 86 400 s averaging period. When required, a simple quadratic sum leads to the Type A uncertainty required for an uncertainty budget computation.

C.2 Type B uncertainty.

Here are the u_b uncertainties taken into account in the uncertainty budget computations, together with the way they are estimated when necessary.

- $u_{b,1}$ observed maximum misclosure. This uncertainty component is an estimation of the stability of the traveling equipment during the campaign. The misclosure $u_{b,1}$ we used here is the actual misclosure between the start and the end of the campaign.
- $u_{b,11}$ position error at reference site. The position of the center of phase of traveling antenna is estimated at opening and closure by using the NRCan PPP software, while for the OP reference station antenna the coordinates of the last G1 calibration are used. Note that this computation is achieved by using GPS data only. This might lead to a small bias on the phase center of the antenna for Galileo signals. We safely choose a conventional value of 70 ps (~ 2 cm) for the position error at the reference site.
- $u_{b,12}$ position error at visited site. At visited sites the position of the center of phase of all antennas is estimated by using the NRCan PPP software. Note that this computation is achieved by using GPS data only. This might lead to a small bias on the phase center of the antenna for Galileo signals. We safely choose a conventional value of 70 ps (~ 2 cm) for the position error at all visited sites.
- $u_{b,13}$ multipath at reference site. We assume in all cases a conventional value of 200 ps, which is in line with some experiment achieved at OP and ORB, especially when using the calibration software developed at OP, where outliers are properly averaged out. (see [2]).
- $u_{b,14}$ multipath at visited site. Same as above.
- $u_{b,21}$ REFDLY (traveling receiver at reference lab). Uncertainty of the measure of the time difference between the reference point of the traveling receiver and the local timescale. The used value is the quadratic sum of an uncertainty value attributed to the Time Interval Counter (TIC) with the standard deviation of the actual measurement (see [3]). When the REFDLY is obtained by summing several individual measurement the uncertainty is increased by quadratic sum as required. We use 220 ps as conservative conventional value.
- $u_{b,22}$ REFDLY (traveling receiver at visited lab). Same as above. This is possible because the TIC we are using for all REFDLY measurements is traveling along with the OP GNSS stations.
- $u_{b,31}$ REFDLY uncertainty of the GNSS reference station to its local timescale. Computed similarly as $u_{b,21}$. This term can be set to 0 when the GNSS reference station has been recently calibrated, the uncertainty of REFDLY being already included in the conventional uncertainty decided by the CCTF WG on GNSS.
- $u_{b,32}$ REFDLY uncertainty (at visited lab) of the link of the visited station to its local UTC(k). Computed similarly as $u_{b,21}$. When this delay is measured and the $u_{b,32}$ is taken into account, the local distribution system can be modified afterwards without loosing the calibration of the local GNSS station, provided the new REFDLY is taken into account afterwards
- $u_{b,41}$ uncertainty of the antenna cable delay at reference station. The chosen value here is based on a comprehensive study which is available in reference [4].
- $u_{b,42}$ uncertainty of antenna cable delay at visited station. Same as just above. When for some reason the antenna cable of the traveling system is changed during the campaign, $u_{b,42}$ is typically obtained from the quadratic sum of the uncertainty of the antenna cable delay actually used at the visited station and the uncertainty of the antenna cable delay of the traveling equipment.

- $u_{b,43}$ uncertainty of the antenna cable delay at visited station. Same as $_{b,41}$.
- $u_{b,SYS}$: Quadratic sum of all type B uncertainties above.

C.3 Combined uncertainty.

- u_{CAL0}: Quadratic sum of u_a and $u_{b,SYS}$. This uncertainty is for the link between the calibrated station and the reference station, without taking into account the uncertainty of this reference station. Note finally that, in our computation, P3 uncertainty values are not based on a linear combination of P1 and P2 uncertainty values but estimated in a similar way as for P1 and P2. And this is also the case for E3 (resp. B3) uncertainty values, which are computed in a similar way as E1 (resp.B1C) and E5a (resp. B2a) uncertainty values.